

Investigation of a model FRET system with multiple donors and acceptors. Allowing validation of data interpretation for studies of cells.

A thesis submitted in partial fulfilment of the requirements of Nottingham Trent University for the degree of Master of Philosophy

William George Austin Gumbs

September 2011

Abstract: In this study the foundations are laid for using a fluorescence microscopy system to view multiple fluorescent species in mammalian cells as a possible technique in investigating the oligomers status of GPCRs. The system utilises spectrally resolved intensity, anisotropy and lifetime measurements. All these techniques are proven to be useable and comparable to the literature. Its weaknesses such as illumination intensity are recognised and its more novel capabilities are utilised. Cho cells are imaged using a confocal microscope and the plasmid sequences providing them with fluorescence through YFP and CFP are established to be correct. In the pursuit of fine tuning the microscope system to allow the live cells images to be taken and any FRET recognised, a model system from the literature is examined. However this turns out to be a fascinating system all of its own; the calculations lead to conclusions that the FRET occurring are in fact predicting inner filter effects along with other unidentified processes. This study looks at why this is the case.

This work is the intellectual property of the author (Note: if there are other owners of the IP, as a consequence of any statement issued under paragraph 12 of Section 14A, they must also be named here). You may copy up to 5% of this work for private study, or personal, non-commercial research. Any re-use of the information contained within this document should be fully referenced, quoting the author, title, university, degree level and pagination. Queries or requests for any other use, or if a more substantial copy is required, should be directed in the owner(s) of the Intellectual Property Rights.

Contents

Abbreviations	4
<u>1. Introduction</u>	7
1.1 GPCR's	7
1.2 Efficacy	9
1.3 Investigating Dimers and Oligomers	10
1.4 Fluorescence	12
1.5 Lifetimes	15
1.6 AB-plots	16
1.7 Anisotropy and Enumeration	18
1.8 Dimers	18
1.9 The Model System	19
<u>2. Methods</u>	21
2.1 Quenching	21
2.2 SDS Micelles Aqueous	21
2.3 Anisotropy	21
2.4 AOT Reverse Micelles	21
2.5 Spectrally Resolved Microscope System	22
2.6 Dye Stocks	24
2.7 Cell Work	24

<u>3. Results</u>	26
3.1 Quenching AB plots	26
3.2 Spectra of Fluorophores	30
3.3 FRET Efficiencies	35
3.4 Cell Work	37
3.5 Anisotropy	40
<u>4. Discussion</u>	42
4.1 Initial Data	42
4.2 Cell work	43
4.3 Moving on to the model system	44
4.4 No FRET	45
4.5 Why no FRET	48
<u>5. Conclusion</u>	59
5.1 The microscope system	59
5.2 The model system	59
5.3 Why the model system is broken	59
<u>References</u>	61

Abbreviations

Å: angstrom

A: the average intensity of the emission wave

a: the average intensity of the excitation wave

A1R: Adenosine A1 receptor

AOT: Bis(2-ethylhexyl) Sulfosuccinate Sodium Salt

arb. unit: Arbitrary unit

b: the difference between its peak intensity and the average of the excitation wave

B: the difference between its peak intensity and the average of the emission wave

BRET: bioluminescence resonance energy transfer

ca: concentration of the acceptor

CCD: Charge-coupled device

cd: concentration of the donor

CFP: Cyan fluorescent protein

Cho: Chinese Hamster Ovaries

CMC: critical micelle concentration

CO₂: Carbon Dioxide

DPCPX: 8-Cyclopentyl-1,3-dipropylxanthine

E: FRET efficiency

EDTA: Ethylenediaminetetraacetic acid

ES: Eosin Y

Fl: Fluorescein

FPS: Fluorescent proteins

FRET: Förster resonance energy transfer

GABA: gamma-aminobutyric acid

GABAb1: gamma-aminobutyric acid B1 receptor

GABAb2: gamma-aminobutyric acid B2 receptor

GDP: guanosine diphosphate

GPCRs: G protein coupled receptors

GTP: guanosine triphosphate

G α : g protein alpha subunit

G β : g protein beta subunit

G γ : g protein gamma subunit

I_d: spectra for lone fluorophore

I_{da}: unmixed spectra for fluorophore

KCl: potassium chloride

K_{nr}: rate of non-radiative decay

LED: light emitting diode

mGluR: metabotropic glutamate receptors

NaOH: sodium hydroxide

PBS: Phosphate buffered saline

r : the distance between the donor and acceptor

R_0 : Förster distance

RB: Rhodamine B

RET: resonance energy transfer

S_0 : singlet ground

S_1 : first electronic state

S_2 : second electronic state

SDS: Sodium dodecyl sulfate

T_1 : first triplet state

UV: ultraviolet

ω : modulation frequency

YFP: Yellow fluorescent protein

Γ : emissive rate of the fluorophore

ϵ_a : molar absorptivity of the acceptor concentrations of donor

ϵ_d : molar absorptivity of the donor

τ : lifetime

τ_{da} : lifetime of donor with acceptor

τ_d : lifetime of donor without acceptor

Φ : phase delay

ω : angular frequency

Investigation of a model FRET system with multiple donors and acceptors. Allowing
validation of data interpretation for studies of cells.

1. Introduction

The purpose of this study is to investigate the proposed FRET system in the Jiang (Jiang and Goedel, 2008) paper titled: "Fluorescence properties of systems with multiple Forster transfer pairs" does not in fact have significant levels of FRET. They claim their systems of fluorophores contained in reverse micelles have a significant level of FRET allowing them to verify the mathematical model they have created to predict the fluorescence intensity of fluorophore mixtures with FRET occurring and it was intended that this system would be used to validate ours in regards to FRET measurement. However we show that although their model predicts the intensities of the mixtures well, their assumption that FRET is occurring is incorrect according to our lifetime data. Analysis based on the absorbance data suggests that the perceived FRET is in fact due to intensity changes caused by inner filter effects.

1.1 GPCR's

G protein-coupled receptors (GPCRs) are the largest class of mammalian cell membrane receptors; with more than 800 different subtypes. Their primary function is the transduction of extracellular stimuli into intracellular signals. GPCRs are sometimes known as seven transmembrane receptors, this is due to the fact GPCRs contain seven cell membrane spanning helices, GPCRs have an extracellular N-terminus and intracellular C-terminus. The intracellular signals are produced by the interaction of the GPCRs intracellular domains with heterotrimeric G proteins. GPCRs respond to a great many extracellular stimuli including odorants, neurotransmitters, light, hormones, chemokines, lipids, peptides and amino acids. Each heterotrimeric G protein is made up of α , β and γ subunits. At least 18 different $G\alpha$ proteins have been shown to couple to GPCRs. At least five types of $G\beta$ and 11 types of $G\gamma$ have been identified with which to form heterotrimeric G proteins with the $G\alpha$ subunit (Emmanuel, 2003; Wong, 2003). GPCRs are present eukaryotes and this includes, yeast, bacteria, plant and nematodes as well as animals, which suggests they had a relatively early evolutionary

origin. The ligands of GPCRs tend to bind to the transmembrane domains of the GPCRs but some GPCRs are activated by cleavage of part of their extracellular domain. This causes a conformational change of the receptor. The activated GPCR prompts the $G\alpha$ subunit of the coupled G protein to exchange the guanosine diphosphate (GDP) which is bound to it, for a guanosine triphosphate (GTP) molecule, this activates the G-protein heterotrimer. The activated G protein disassociates into the $G\alpha$ monomer and $G\beta$ - $G\gamma$ dimer, the $G\alpha$ subunit activates the downstream pathway although sometimes the $G\beta$ - $G\gamma$ dimer can have its own activation effects. Depending of the G protein coupled to the GPCR a wide variety of downstream signalling pathways can be activated. The $G\alpha$ monomer has GTP to GDP hydrolysis capability which eventually returns the $G\alpha$ subunit to its inactive form, at which point it reassociates with the $G\beta$ - $G\gamma$ dimer, reforming the inactive G protein. There is also research showing G protein independent activation of downstream signalling in some GPCRs (Gsandtner et al., 2005). Desensitisation in GPCRs is achieved through internalisation by arrestin binding (Ferguson, 2001). More than 30% of pharmaceuticals act on GPCRs (Schlyer and Horuk, 2006) and therefore understanding their pharmacology is important to the field of drug development.

One aspect of GPCR pharmacology which can affect how they function, is oligomer formation (Maggio et al., 1993; Jordan and Devi, 1999; Marrero M et al., 1999; Rocheville et al., 2000a; Canals et al., 2003; Carrillo et al., 2003; Dinger et al., 2003; Hoffmann et al., 2005; Lopez-Gimenez et al., 2007; Jiang et al., 2009). Originally believed to function as monomers, evidence in recent years has shown that for some GPCRs oligomer states are crucial to their function. One example of this behaviour found in gamma-aminobutyric acid (GABA) receptors. The two types: $GABA_{b1}$ and $GABA_{b2}$ receptors must form a dimer to create a functional receptor (Jones et al., 1998; Kaupmann et al., 1998; Kuner et al., 1999). Whether GPCR's function as monomers or oligomers, both homo and hetero, may significantly affect how cells respond to drugs which act on GPCRs. Some have been shown to form complexes where one monomer provides the ligand binding site and another within the complex provides the connection to the downstream part of the signalling pathway, allowing a ligand which cannot bind directly to the GPCR's of a certain pathway to still activate it by co-opting the transduction mechanism of another, other GPCRs show a change in the efficacy of their ligands

(Maggio et al., 1993; Jones et al., 1998; Kaupmann et al., 1998; Jordan and Devi, 1999; Kuner et al., 1999; Rocheville et al., 2000a; Carrillo et al., 2003).

1.2 Efficacy

The efficacy of a ligand-receptor complex is a measure of the ability of that complex to produce the maximum signalling response which would be produced by a complex of the receptor and its endogenous agonist; an efficacy of 100%. A full agonist will have the same effect as the endogenous agonist at the same concentration; some molecules are super agonists meaning they create greater signalling response at the same concentration thus an efficacy more than 100%. Partial agonists have reduced efficacy as compared to the endogenous agonist. True antagonists have no effect on the basal activity for receptor and thus would have 0% efficacy. Finally inverse agonists reduce the basal activity of receptor. The efficacy is separate from affinity or how strongly a ligand binds to receptor, thus molecules with higher affinity than the endogenous ligand can displace it and alter the level of the signalling from receptor, molecules of the lower affinity can also compete with the endogenous ligand however they have to be in much higher concentrations. But in the context of drug development molecules with the right efficacy and high affinity are sought. Being able to ascertain which GPCR's function as oligomers, what the component parts of that oligomer are and how oligomer formation affects receptor function, will allow better understanding of drugs and their effects. This, it is hoped, should therefore lead to better drug targeting, which should provide better treatments with fewer side effects.

The adenosine A₁ receptor (A₁R) is a GPCR; which is present in most tissues of the body including the central nervous system where it is one of the most abundant GPCR's (Dunwiddie and Masino, 2001) and vasculatory (Tawfik et al., 2005) systems. Its effects are generally inhibitory. It will be used in our study as a model oligomer forming GPCR. A₁R has been shown to form heterodimers with dopamine D₁ receptors (Franco et al., 2000; Ginés et al., 2000; Cao et al., 2006), P₂Y₁ purinergic receptors (Yoshioka et al., 2001, 2002a, 2002b), mGluR1 α (Ciruela et al., 2001) and Histamine H₁ receptors amongst others. There is also biochemical data supporting the existence of A₁R homo-dimers (Franco et al., 2000; Yoshioka et al., 2002a). The majority of studies into GPCR oligomers have looked at dimers and it is likely that this is due to the fact that most of the current methods for studying GPCR

oligomers can show the interaction of two proteins but have difficulty enumerating higher oligomers.

1.3 Investigating Dimers and Oligomers

Many techniques have been utilised to investigate whether these dimers form and have shown they do. Western blots showed some of the first evidence that dimers existed. In a western blot the proteins are separated by gel electrophoresis depending on primary structure length (if the protein is first denatured) or by tertiary structure. The proteins are transferred from the gel to an absorptive membrane (e.g. nitrocellulose). This membrane is then probed using anti-bodies specific to part of the target protein or an epitope tag (epitope-tagging is the addition of a peptide sequence which has a very high affinity to certain antibodies; allowing these antibodies to be used to detect the protein, the polyhistidine-tag is a frequently used tag), which are themselves labelled, or another labelled anti-body will be added which binds to the initial antibody to allow detection. Western blots are often used in conjunction with co-immunoprecipitation using an antibody to a known protein of the complex. This anti-body is bound to something that will allow it to be removed from the solution when desired such as an agarose or magnetic bead. Once the target has sufficient time to bind this allows the antibody and target to be brought out of the solution. The target protein is then eluted from the antibodies. The solution can then be tested for other proteins thought to be bound. Any protein present, other than the original target, must have been bound to the original target.

Several studies using both immunoprecipitation and western blots have shown dimers and oligomers in GPCRs (Nimchinsky et al., 1997; Salim et al., 2002; Xu et al., 2003). A key problem with these methods is that the solubilisation step can cause the formation of reactive groups which could allow receptors which are not natively dimers to bind however the controls present in certain studies suggests this is not the case in at least some of the GPCR's which have been studied (Jordan and Devi, 1999).

Functional complementation and transactivation methods have also been used. Here a cell line is altered so that it produces two version of GPCR's; in one version the ligand binding domain is inactivated, in the other the signal transducing domain is inactivated. Dimerisation allows each to

utilise the unaltered portion of the partner to form a functional receptor, and this has been shown to occur for several GPCRs (Rocheville et al., 2000b; Carrillo et al., 2003). However, this prevents observation of any effects that require the receptor to be intact. Techniques utilising bioluminescence resonance energy transfer (BRET) and FRET have also been used. For resonance energy transfer to occur the emission spectra of the donor must overlap the excitation spectra of the acceptor fluorophore. In BRET the donor is luminescent whereas in FRET the donor is fluorescent (e.g. GFP). In both techniques fusion proteins of the GPCRs and the donor are present in the cell, along with the fusion proteins of the GPCRs and the acceptors. To show dimer or oligomerisation RET must be seen, it only occurs when the molecules are less than 10nm apart. The donor is activated by light in the case of FRET and by addition of the enzyme substrate in BRET. If light is emitted by the acceptor then RET has occurred suggesting the GPCRs are in close proximity, likely as part of a dimer or oligomer.

Several studies have used BRET and FRET to show dimerisation or oligomerisation (Rocheville et al., 2000a; Cheng and Miller, 2001; Ramsay et al., 2002; Dinger et al., 2003; Fiorentini et al., 2003; Pfeiffer et al., 2003). We intend to work on the technology required to view both homo and hetero A₁R oligomers, in live cells and attempt to elucidate how many proteins are present within these complexes, using a combination of fluorescence lifetime imaging, static and dynamic anisotropy, and imaging spectroscopy. Fluorescence resonance energy transfer (FRET) or Förster resonance energy transfer causes changes in anisotropy (Gautier et al., 2001; Lidke et al., 2003; Bigelow et al., 2004) and it is possible to use this to provide information on the likely number of fluorophores in a complex (Yeow and Clayton, 2007). Spectrally resolving the image will allow us to examine the spectrum, lifetime and anisotropy data from each pixel within the image. This combination will allow the location and identification of different species of fluorophore in our systems.

The fluorophores in the system described in the Jiang paper are contained in reverse micelles. Micelles are formed when the concentration of a surfactant is above its critical micelle concentration (CMC) and the solution temperature is more than the Krafft temperature. Micelles are generally shaped like a sphere or an ellipsoid and can also form cylinders. (Goel et al., 2010) In a non-ionic surfactant the micelle can be made of 1000 or more surfactant molecules however if it's ionic then it

will tend to be less than 100 because it is limited by electrostatic repulsion between the head groups. The location of molecules dissolved in a micelle is also affected by whether the surfactant is ionic or non-ionic, micelles comprised of a non-ionic surfactant are not affected by electrostatic attractions, in an ionic surfactant however these electrostatic attractions cause the local environment of the Stern layer to be very complex, due to the charged head groups and counter ions occupying a restricted space.(De et al., 2005) In a micelle of surfactant dissolved in water, the hydrophobic tails cluster in the centre of the sphere/ellipsoid of surfactant molecules, this hydrocarbon interior is like a droplet of oil, the hydrophilic heads are presented to the water. Due to the fact that the inside of the micelle is like a non-polar solvent, species which normally wouldn't dissolve in water, can be dissolved in water containing surfactant as they can locate themselves within the micelle. If a surfactant is used in a mixture of water and a non-polar solvent, then a reverse micelle can be formed. A reverse micelle has the hydrocarbon tails on the outside and water and the hydrophilic head groups on the inside, forming an aqueous core. This will allow water-soluble substances to be dissolved into a non-polar solvent. This localisation of dissolved molecules to the micelles causes them to have a high local concentration compared to if they were dissolved throughout the solvent. The size and morphology of a reverse micelle varies depending on the presence of other compounds such as salts and the water to surfactant ratio.(Vasquez et al., 2011)

1.4 Fluorescence

Fluorescence is the absorption and emission of energy in the form of light. A photon (in special cases two) is absorbed by the fluorophore, causing one of its electrons to move into an excited orbital. This electron is paired by opposite spin to an electron in the ground state orbital. This means returning to the ground state is spin allowed and it occurs via the emission of a photon. If this occurs without intersystem crossing it is fluorescence. If intersystem crossing has occurred then the light emission is phosphorescence. Intersystem crossing is where a molecule in the S_1 state undergoes a spin conversion to the first triplet state T_1 . This is often shown using a Jablonski diagram as in Figure 1. In the diagram S_0 , S_1 and S_2 represent the singlet ground, first and second electronic states respectively. The fluorophore can exist in a number of the vibrational energy levels at each of these electronic energy levels. The vertical lines illustrate transitions between states. Although excitation of a

fluorophore is normally to a higher vibrational level of either S_1 or S_2 , molecules in condensed states rapidly relax to the lowest vibrational energies of S_1 . This generally occurs within 10^{-12} s and is called internal conversion. This is shorter than the typical fluorescence lifetime which is nearer 10^{-8} s, thus fluorescence emissions generally reflect the lowest energy vibrational energy state of S_1 .

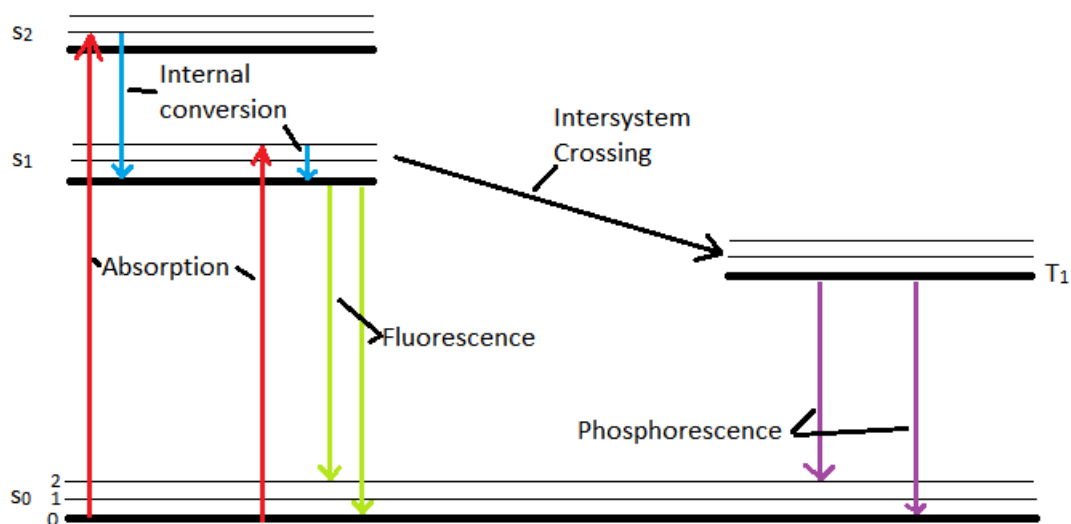


Figure 1: Jablonski Diagram

There are several important properties of fluorescence including intensity, wavelength, lifetime and anisotropy. Generally fluorophores are organic molecules such as the rhodamines, fluorescein, anthracene, perylene and fluorescent proteins (FPs). Each fluorophore has characteristic absorption and emission spectrum. The emission spectrum is of a longer wavelength than the absorption spectrum and this change is called the Stokes shift. Large Stokes shifts are useful as it allows the signal from the fluorophore to be easily separated from that of the excitation source. Another important property in a fluorophore is its quantum yield which is the ratio of the number of photons emitted to the number of photons absorbed. Quantum yield can also be expressed as Equation 1.

Equation 1:

$$Q = \frac{\Gamma}{\Gamma + K_{nr}}$$

Where Q is quantum yield, Γ is emissive rate of the fluorophore and K_{nr} is the rate of non-radiative decay. This is related to Equation 2 which defines lifetime.

Equation 2:

$$\tau = \frac{1}{\Gamma + K_{nr}}$$

Where τ is lifetime and the two combined rates govern its duration.

When a system contains multiple fluorophores; they can undergo a process called Förster resonance energy transfer (FRET). If the emission spectrum of one fluorophore -referred to as the donor- overlaps with the absorption spectra of another fluorophore, referred to as the acceptor, then energy can be transferred from the donor when it is in an excited state to the acceptor; which is in ground state resulting in the acceptor emitting a photon. However no photon passes between the pair, the energy is passed by a long-range coupled dipole-dipole interaction. The degree of energy transfer is affected by the magnitude of the spectral overlap between the donor's emission spectrum and the acceptors absorption spectrum, the quantum yield of the donor, the relative orientations of the donor and acceptor's transition dipoles and the distance between the two fluorophores. The distance between donor and acceptor which results in 50% FRET is referred to as the Förster distance and is generally between 20 and 60 Å. The rate of energy transfer can be determined with Equation 3.

Equation 3:

$$k_{\tau}(r) = \frac{1}{\tau_D} \left(\frac{R_0}{r} \right)^6$$

Where $k_{\tau}(r)$ is the rate energy transfer, τ_D is the lifetime of the donor without acceptor, R_0 is the Förster distance, and r is the distance between the donor and acceptor. This formula also allows the amount of FRET in a system to be used to determine the distance between the donors and acceptors. This is often used to determine the distance between labelled biological molecules. FRET can occur between two fluorophores of different types and this is referred to as heterotransfer, it can also occur between two fluorophores of the same type and this is referred to as homotransfer. Homotransfer can be detected by a decrease in anisotropy. Heterotransfer causes a decrease in donor intensity and lifetime, due to the effective quenching of the donor by the acceptor.

1.5 Lifetimes

Phase and modulation lifetimes are recovered when using frequency domain techniques to measure lifetime. To obtain frequency domain data the intensity of the excitation source is modulated, the modulation of the excitation source is given by b/a , a represents the average intensity and b represents the difference between the peak intensity and the average. Due to the modulation of the excitation source intensity, emission intensity is also modulated, its modulation is calculated by B/A where A is its average intensity and B is the difference between its peak intensity and the average. The ratio of B/A and b/a gives the demodulation factor m , although this is generally referred to as the modulation. The modulated emission signal also has a phase delay (ϕ) and this is referred to as the phase angle, and this is the time difference between occurrence of the excitation peaks and emission peaks (Figure 2).

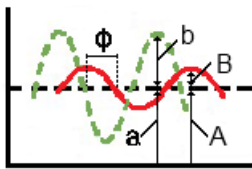


Figure 2: Diagram showing the values required to calculate modulation and phase lifetime on a pair of sine waves, green shows the modulation of the excitation light and red the modulation of the emission light.

The phase angle and modulation can then be used to calculate the apparent phase (τ_ϕ) and modulation (τ_m) lifetimes using *Equation 5* which is a rearrangement of *Equation 4* and *Equation 7* which is a rearrangement of *Equation 6*.

Equation 4:

$$\tan \phi = \omega \tau_\phi$$

Equation 5:

$$\tau_\phi = \omega^{-1} \tan \phi$$

Equation 6:

$$m = \frac{1}{\sqrt{1 + \omega^2 \tau_m^2}}$$

Equation 7:

$$\tau_m = \frac{1}{\omega} \left[\frac{1}{m^2} - 1 \right]^{1/2}$$

Where $\omega = 2\pi x$ and x is the modulation frequency. The excitation source is generally modulated at a frequency of 10-200MHz depending on the fluorophores lifetime and the system being used.

Increasing the frequency of modulation increases the phase angle and decreases the modulation. (Lakowicz, 1999)

1.6 AB-plots

AB plots are also known as phasor plots and polar plots. AB plots make the analysis of multi exponential decays easier by providing a graphical representation of the phase and modulation lifetime data from a sample, which has clearly identifiable features related to composition of the sample and the interactions of its parts. It also allows data which would be clipped due to ill-behaviour in the classical representations to be included and interpreted. In a sample with a single species the data points will cluster around a point on the one to one semicircle (Figure 3).

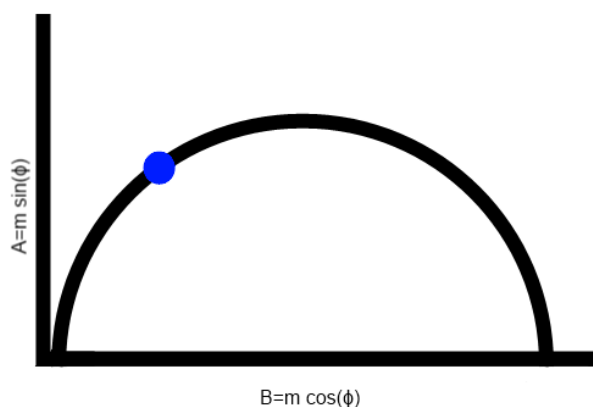


Figure 3: Illustration of an AB plot with a single fluorophore with a single lifetime.

If the sample has two species, which do not interact, with different lifetimes, the points on the plot will form a straight line between the two points on the one to one semi-circle representing the lone lifetimes (see Figure 4). The position of the point on this line represents how much of the signal is due to each fluorophore, for instance a point in the middle of A and B would have 50% of the light contributing to its intensity from A and the other 50% from B.

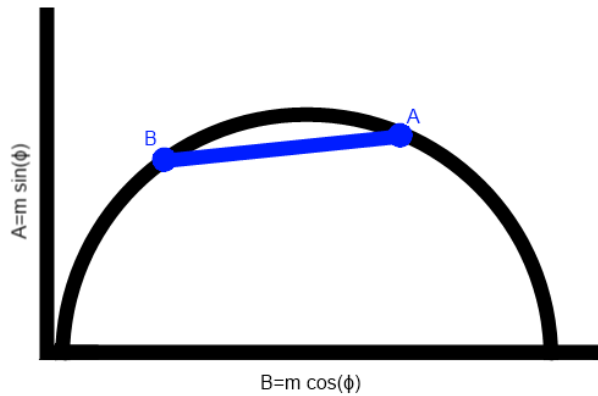


Figure 4: Illustration of an AB plot with two fluorophores with different lifetimes.

In a sample with 3 or more species each with a distinct lifetime and no interaction between species then the expected distribution of points lies in a 2D space with the points corresponding to the lone lifetimes of the species as the corners (Figure 5). As you move along the semicircle the lifetimes decrease for instance in Figure 4, B has a longer lifetime than A. Increasing the frequency of modulation shifts the data points along the semicircle to the left.

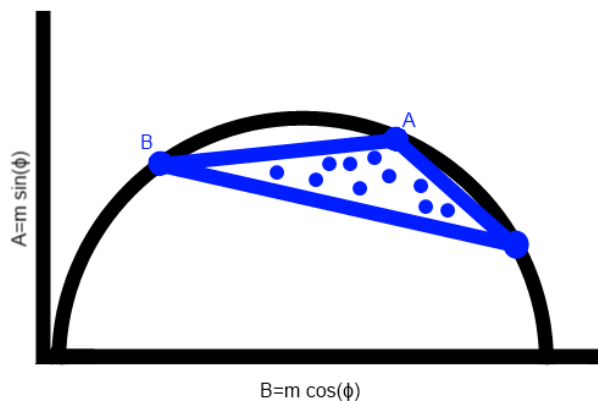


Figure 5: Illustration of an AB plot with three fluorophores with different lifetimes and linear mixing.

Where the species do interact (e.g. FRET) the points will move off the lines connecting the lone species and potentially out of the triangle space formed by connecting the corners represent the lone fluorophores (Hanley et al., 2001, 2002, 2006; Clayton et al., 2004; Hanley and Clayton, 2005; Redford and Clegg, 2005; Digman et al., 2008; Verveer and Hanley, 2009; Zhou et al., 2009).

1.7 Anisotropy and Enumeration

For FRET to occur the molecules have to be in close proximity (<10nm) thus the occurrence of FRET between the FPs of two or more GPCRs shows their colocalisation. A specific type of FRET is homotransfer which is where the energy transfer occurs between two fluorophores of the same species and this can be used for the enumeration of an oligomer. Anisotropy is a measure of the difference in the polarisation of the light emitted by a fluorophore and the light which was used to excite it and homotransfer causes a reduction in anisotropy and is more likely in oligomers due to the monomers close proximity to one another. Photobleaching stops the affected fluorophores from participating in FRET events and thus looking at the changes in the anisotropy values as a sample is photobleached may potentially allow us to enumerate the GPCR oligomers. (Yeow and Clayton, 2007)

1.8 Dimers

Dimers are formed by certain fluorophores. In xanthene dyes strong electrostatic and dispersion interactions facilitate this. The dimers are favoured by high concentration and lower temperature. These dimers tend to absorb light differently than the monomers and thus can change the absorbance spectra. They also have the potential to change the fluorescence spectra. However many homodimers are non-fluorescent as they self-quench due to dipole alignment and intersystem crossing and internal conversion when the aggregates are in the excited state. This leads to concentration and temperature dependent changes in the dyes quantum yield, because of the dimer-monomer equilibrium shift. Salts can also enhance this dimer formation; AOT is an anionic surfactant and may act in a similar way.

1.9 The Model System

The Jiang paper looked at mixtures of dyes as they pertain to labelling (Battersby et al., 2000, 2002). They comment on the fact that using multiple dyes in different concentrations allows many different objects to be labelled with the same dyes if their intensities mix linearly. They then explain that the influences of FRET will change the spectral signal from the dyes and thus to use multiple dye labelling the effects of FRET have to be taken into account. The paper looks at producing a mathematical model which given the concentration of the original dyes and both their emission and absorption spectra will predict the intensities with FRET taken into account. They attempt to take into account the probabilities the dye molecules will be excited and the probability of losing the excitation energy by emission, quenching, FRET and non-radiative decay. To test the two models (One model is based on the Stern-Volmer equation and the other is based on a simple exponential function) a three dye system comprising of fluorescein, eosin and rhodamine B was selected because they are water-soluble and had been used in previous investigations of FRET. This system was believed to be sufficiently chemically stable and to have significant overlap between the excitation and emission spectra of the dyes. They state that to test the models, synthesis of solid particles is not required, high local concentration and low absorbance is sufficient. To achieve this, the dyes were put into reverse micelles of AOT with aqueous cores suspended in isooctane. They note however that the use of a reverse micelle system may affect the accuracy of their predictions due to the fact that the distribution of the dye molecules is not exactly the same as it would be in a solution. The dyes attached to the micelle wall are not surrounded by dye molecules on all sides. Analytical grade fluorescein, eosin and rhodamine B were used, the isooctane was 99.5% pure and the AOT was 98% pure. The dyes were dissolved in purified water and then added to AOT dissolved in isooctane to form the required concentrations, 4% of the solutions were water and dye and the other 96% with isooctane with dissolved AOT. These solutions were then sonicated to ensure homogeneous mixing. The fluorescence spectra were taken using a Perkin Elmer LS 50B luminescence spectrometer and they were excited at 494 nm. Self-quenching is seen at the concentrations used. The key line which refers to FRET occurring in their systems is as follows:

“Compared to the spectra with single dye systems, the decreased emission of FL and increased emission of ES and RB demonstrate efficient fluorescence resonance energy transfer between dyes in reverse micelles.”

We believe this statement to be a misinterpretation of the data. While both models provide fairly accurate predictions of the experimental data, we show that the dyes in an experimental system do not appear to undergo FRET and therefore the suggestion in the paper that these methods can be used to predict the intensities of systems which do have FRET is invalid.

2. Methods

2.1 Quenching

Potassium iodide was used as a collisional quencher. A solution of quencher at twice the required end concentration and a solution of the dye at double the required concentration were made and these were then added in a 1:1 ratio to produce the required concentrations. Potassium iodide solutions were made up fresh on the day.

2.2 SDS Micelles Aqueous

For the SDS micelles the SDS in each of the solutions was at a concentration of 55 mM. The dyes and SDS were added as the required weight of powder and then made up to the required volumes in volumetric flasks. For the buffered systems sodium carbonate-bicarbonate (lab stock, original concentrations unknown) was used to maintain pH 9.5 and sodium hydroxide and potassium chloride buffer for pH 12.9 (25mls of 0.2M KCl with 0.2M NaOH added until the pH was 12.9 at 25.6°C using a Hanna HI 4212 pH meter).

2.3 Anisotropy

A small amount concentrated of rhodamine 6G solutions (170 µl of 0.589mM) was added to give the final solutions a concentration of about 20µM) to 0.00g, 0.76g, 2.38g and 3.06g of glycerol, these were then made up to 5g with deionised water. These were then imaged using our system which has an automatically rotated polariser at the excitation source and a stationary polariser at the emission filter.

2.4 AOT Reverse Micelles

Reverse micelles of iso-octane and bis(2-ethylhexyl)sulfosuccinate sodium salt (AOT) (98% purity, Aldrich Chemistry, CAS:577-11-7) with cores of aqueous dyes were prepared. The fluorescent dyes fluorescein (Purity: "Pure" no percentage given, Acros Organics, CAS:518-47-8), rhodamine B (99% Purity, Acros Organics, CAS: 81-88-9) and eosin Y (Purity 90%, Sigma-Aldrich, CAS:17372-87-1). The dyes were made up in a pH 12.9 buffer (25mls of 0.2M KCl with 0.2M NaOH added until the pH was 12.9 at 25.6°C) to keep fluorescein in its anionic form and to keep the eosin Y in solution. The 10 µM

fluorescein, 20 μ M eosin Y and 40 μ M rhodamine B was used in 0.417M AOT in iso-octane. To make the iso-octane AOT water micelles weight out AOT required for a 0.417M solution onto the analytical balance. Transfer to a volumetric and add \sim 50% of total volume of iso-octane, put on shaker till all AOT has dissolved. Then add iso-octane up to the mark on the volumetric. This is the stock AOT in iso-octane. To create the reverse micelles 4% of the mixture is deionised water/buffer and dissolved dye. Pipette the required volumes of stock dyes and then pipette required deionised water to make the 4%. Fill up to the mark on the volumetric with AOT in iso-octane stock. Sonicate for 5 mins. These were read in a Lambda 25 Spectrometer spectrophotometer (PerkinElmer) for the absorbencies.

2.5 Spectrally Resolved Microscope System

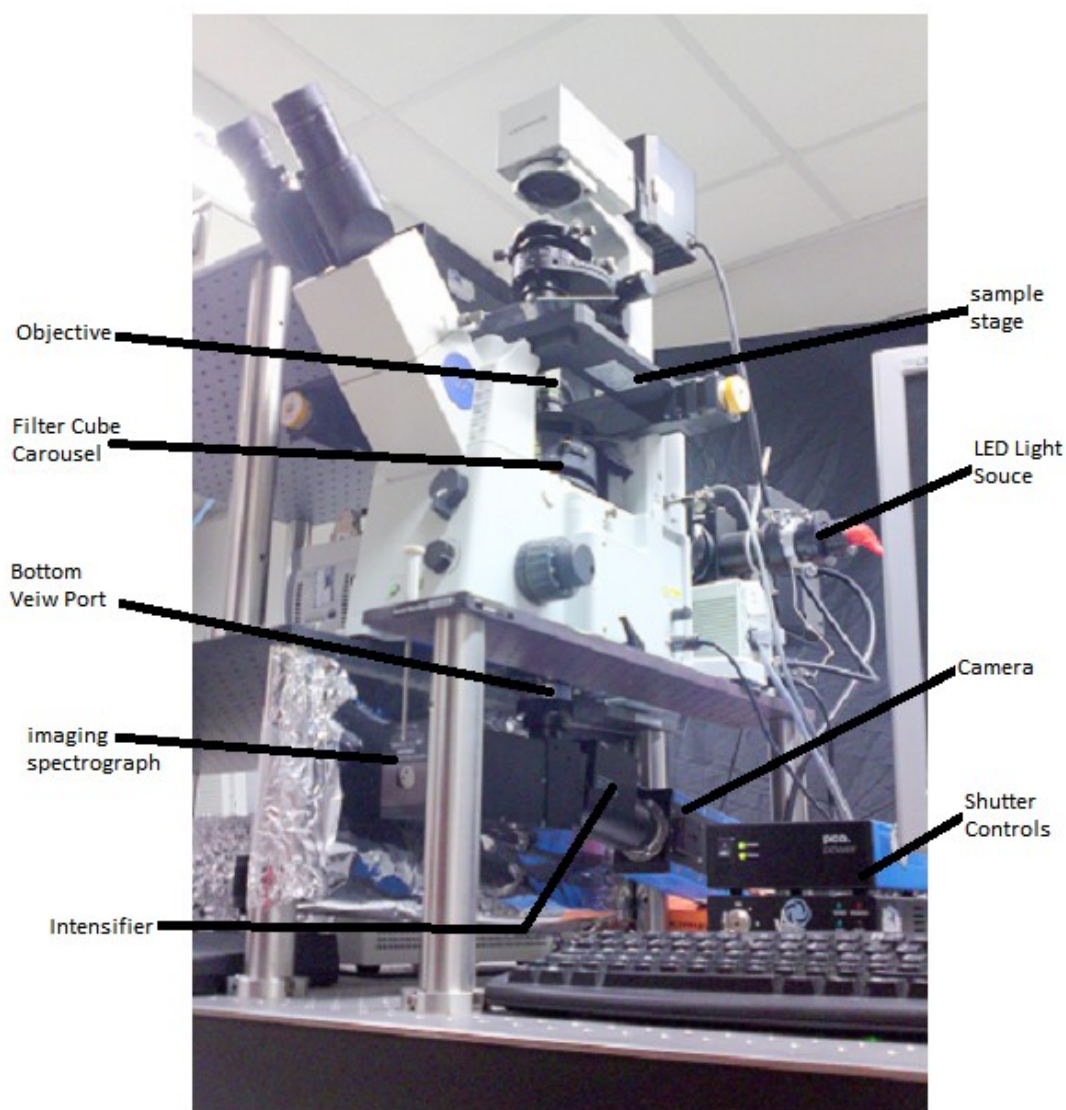


Figure 6: The modified Olympus IX71 fluorescence microscope.

Fluorescence intensity and lifetime was measured in our own system. A modified Olympus IX71 fluorescence microscope (IX71; Olympus UK Ltd, Southall, UK). In order to ascertain the lifetime and spectral data, the microscope has been modified with an imaging system. The imaging system attaches to the bottom view port of the microscope. For illumination either a 470 nm LED (LUXEON III, RS Electronics, UK) was used. The LED was mounted in a fixed housing with a condenser (Cairn Research Ltd, Faversham, UK). The light passes through a polariser (05CA25; Comar Instruments, Cambridge, UK). The linearly polarised light then enters the polarisation rotator (LV2500-OEM; Displaytech Inc., Longmont, CO, USA), which is controlled by the computer. The microscope is fitted with a filter set (Omega Optical Inc., Brattleboro, VT, USA, 450nm DF 55 excitation filter, 485nm DR LP dichroic mirror and 500nm ALP emission filter) and a 20x NA 0.45 objective lens (LUCPLFLN 20x, Olympus UK Ltd, Southall, UK). The samples are contained in a 96 well glass bottomed plates (Nunc 164588, VWR International Ltd, Lutterworth, UK). Which are mounted on an automated XY translational stage (Märzhäuser Wetzlar GmbH & Co. KG, Wetzlar-Steindorf, Germany) controlled by the computer. The light emitted from the sample passes through the emission filter and then a second polariser (05CA25; Comar Instruments, Cambridge, UK) acting as the analyser. From here the light enters an imaging spectrograph (PARISS; Lightform Inc., Hillsborough, NJ, USA), then a modulated image intensifier (II118MD; Lambert Instruments, Leutingewolde, The Netherlands) and is detected with detected with a 14-bit cooled CCD camera (PCO 1600; PCO Computer Optics GmbH, Kelheim, Germany). The intensifier gain was modulated at 60MHz, -8dBm by a signal generator (2023A; Aeroflex, Stevenage, UK).

For fluorescence intensity and lifetime measurements the rotator keeps the exciting light's polarisation parallel to the analyser. When performing anisotropy measurements the rotator allows parallel and perpendicular images to be taken. The rotator is connected to the computer via USB (C8051F320-DK; Silicon Laboratories, Austin, TX, USA). The LED amplitude is modulated by a second signal generator (2023A; Aeroflex) the output the signal generator is amplified (ENI Model 403LA, West Henrietta, NY, USA)) and then combined via a bias tee (8800SMF3-02, Sematron UK Limited, Hampshire, UK) with current from a DC power supply (HP Agilent E3634A, Agilent Technologies UK Limited, Berkshire, UK).

The driving signal is passed through a power resistor network which is in series with the LED this produces a radio frequency modulation of the LED light source. The signal generators are phase locked. Software written in Microsoft Visual Studio C++ Net 2005 and Matlab 2006a runs the system and extracts the phase and modulation lifetimes. The prism allows wavelength information to be obtained about the image. The lights angle of diffraction depends on its wavelength, this means that light of different wavelengths falls on different parts of the CCD camera, this can then be calibrated through the use of a known source such as an Neon lamp, light known to fall on a certain part of the CCD camera can then be attributed a wavelength. This provides us with the spectral information. The lifetimes of the present fluorophores are established through the observation of modulation and

phase change of the emitted light compared to the excitation light.(Verveer and Hanley, 2009)
Rhodamine 6G (Purity 99%, Acros Organics, CAS: 989-38-8) used as a lifetime.

2.6 Dye Stocks

For the stock dyes, dye powder was weighed on the analytical balance directly into a volumetric. This was made up to the mark on the volumetric with deionised water/buffer. Mixed by inversion then sonicated for 5 min. Dye stocks needed to be 100 times as concentrated as the final reverse micelle mixture to allow for dilution.

2.7 Cell Work

The cell line CHO - A1 – YFP was passaged and maintained in Dulbecco's modified Eagle's medium F12 with 9% fetal calf serum, penicillin, streptomycin, L glutamine and neomycin G418 at to maintain selection pressure for the YFP plasmid (this is here on referred to as “growth medium”). The cells were grown in a 37°C incubator at a CO₂ level of 5%. The cells were grown in T75 cell culture flasks. To remove the cell from the flask surface for passage trypsin with EDTA in PBS was used after removing the old growth medium, after incubating for 5 mins; the content of the flask was then poured into a centrifuge tube and the same volume of growth medium was added. This was centrifuged till a pellet was obtained, the liquid in the centrifuge tube was removed and the pellet was resuspended in 10ml of growth medium, a haemocytometer was then used to perform a count of a known volume stained with tryptophan blue. Based on that count sufficient volume to provide 5000 cells was used to seed 20ml of growth medium, which was then added to a new flask.

The cells were viewed using the modified Olympus IX71 system to look for fluorescence from the YFP and a Leica Microsystems Heidelberg GmbH confocal system to view the YFP and a fluorescently labelled agonist (CellAura A-633-AG) which was incubated with them. The HCX PL FLUOTAR 40.0x 0.75NA PH2 objective was used. The 632nm Helium-Neon laser line was used as the excitation source for the agonist and the 488nm Argon laser line was used as the excitation source for the YFP. The Colocalisation of the YFP tagged adenosine A₂R receptors was calculated for the confocal images

using the ImageJ program(Abramoff et al., 2004) and the JACoP plugin(Bolte and Cordelières, 2006).

The images were converted to 8bit greyscale, despeckled and then analysed with JACoP.

The cells were fixed using paraformaldehyde solution (4 g of paraformaldehyde and 6 µl of 10M NaOH was dissolved in 100 ml of phosphate buffered saline (PBS) at 60°C). The cells were grown to a semi-confluent state in a 96 well plate (nunc glass bottomed). The growth medium was removed from the wells and 200 µl of paraformaldehyde solution (cooled to equilibrium with an ice bath) was added to each well. The plate was then incubated for 15 minutes in a 4°C refrigerator. The wells were then washed twice with PBS. Each well was then filled with 200 µl of PBS for storage and imaging. To some of the wells 8-Cyclopentyl-1,3-dipropylxanthine (DPCPX) was added at this point. DPCPX is a potent selective antagonist to the adenosine A₁ receptor and is highly selective of A₁ receptor over the other adenosine receptor forms. The plate was then incubated for 15 minutes in a 4°C refrigerator. Then the agonist was added to the wells which required it. The plate was then incubated for 30 minutes in a 4°C refrigerator.

Samples of the plasmids used to transfect the CHO cell lines we are using for imaging were sent for sequencing. The returned sequences were then aligned using programs from The European Bioinformatics Institute (EBI) website. These sequences were then compared to the desired sequences.

3. Results

3.1 Quenching AB plots

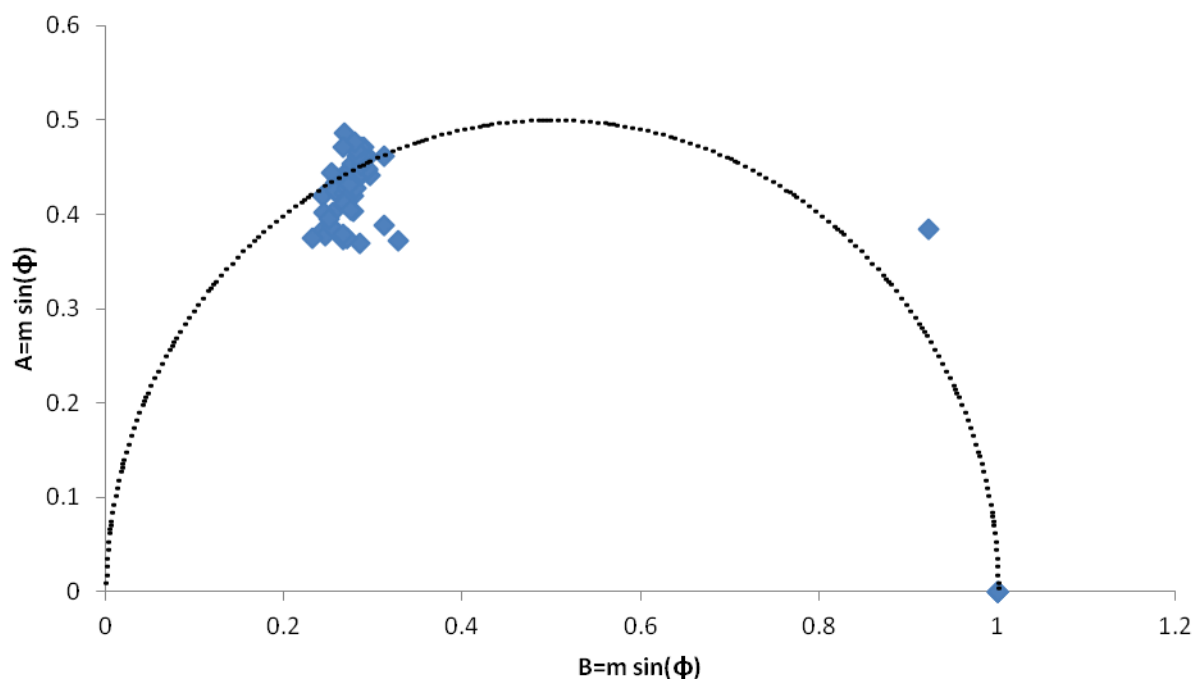


Figure 7: AB plot of 10 μ M rhodamine 6G without potassium iodide quencher.

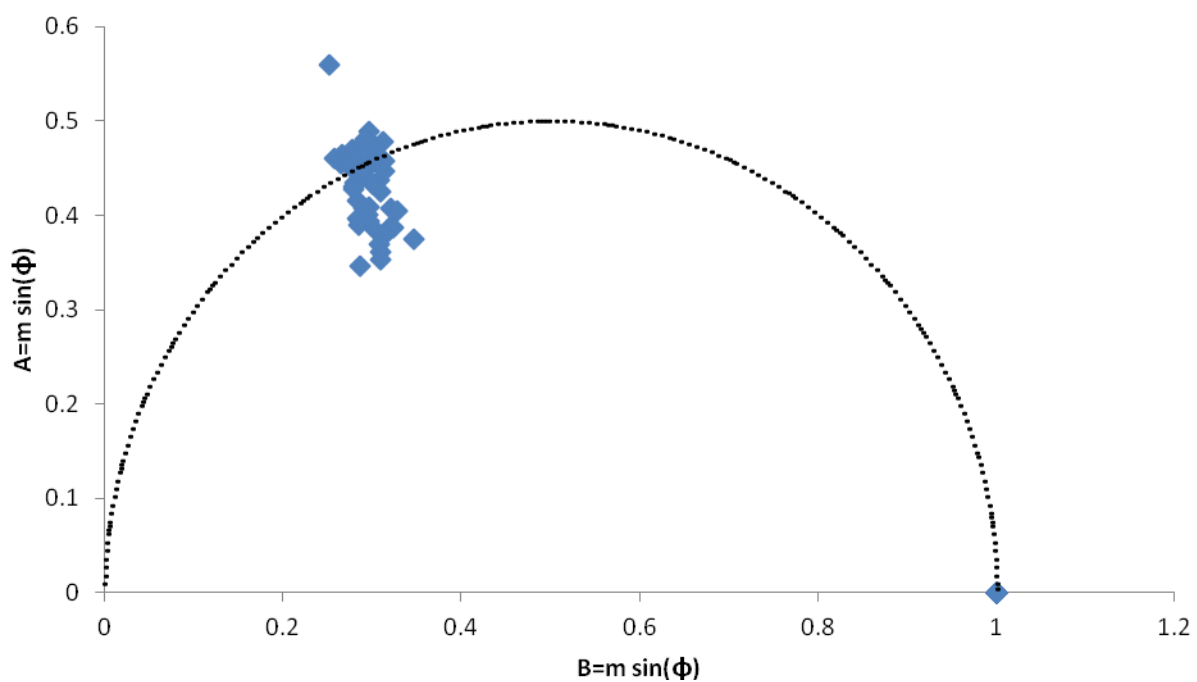


Figure 8: AB plot of 10µM rhodamine 6G with 16mM potassium iodide quencher.

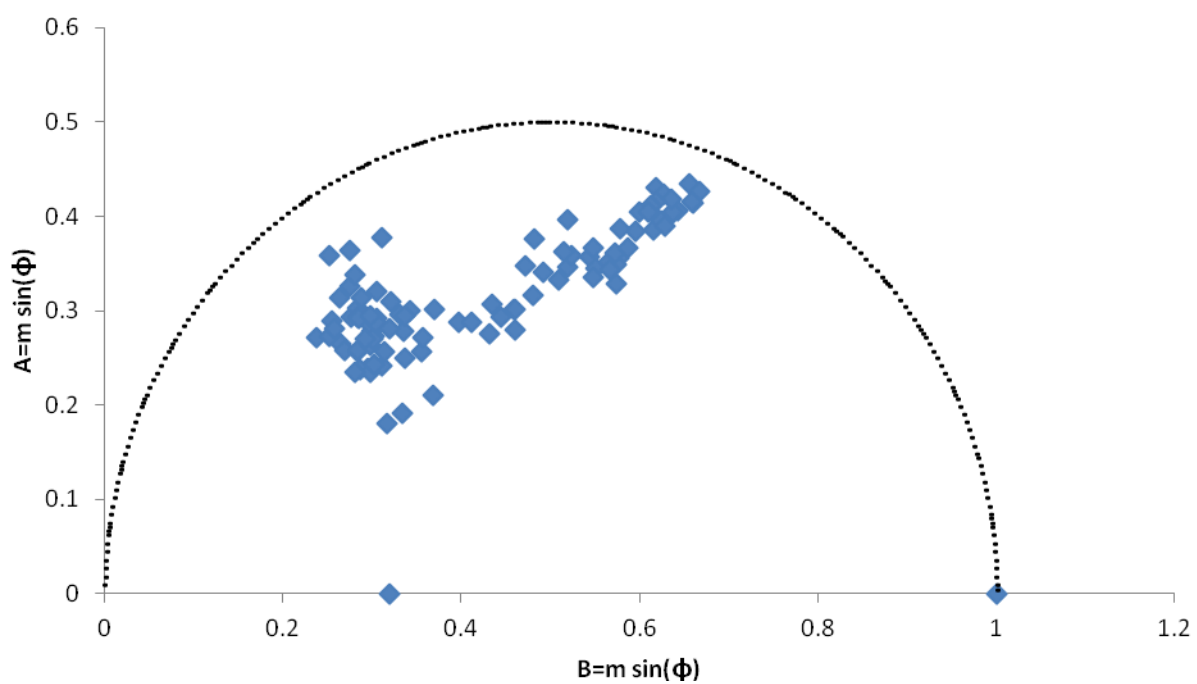


Figure 9: AB plot of 10µM rhodamine 6G with 31mM potassium iodide quencher.

Figure 7, Figure 8 and Figure 9 show little sign of quenching and there is clear evidence of noise.

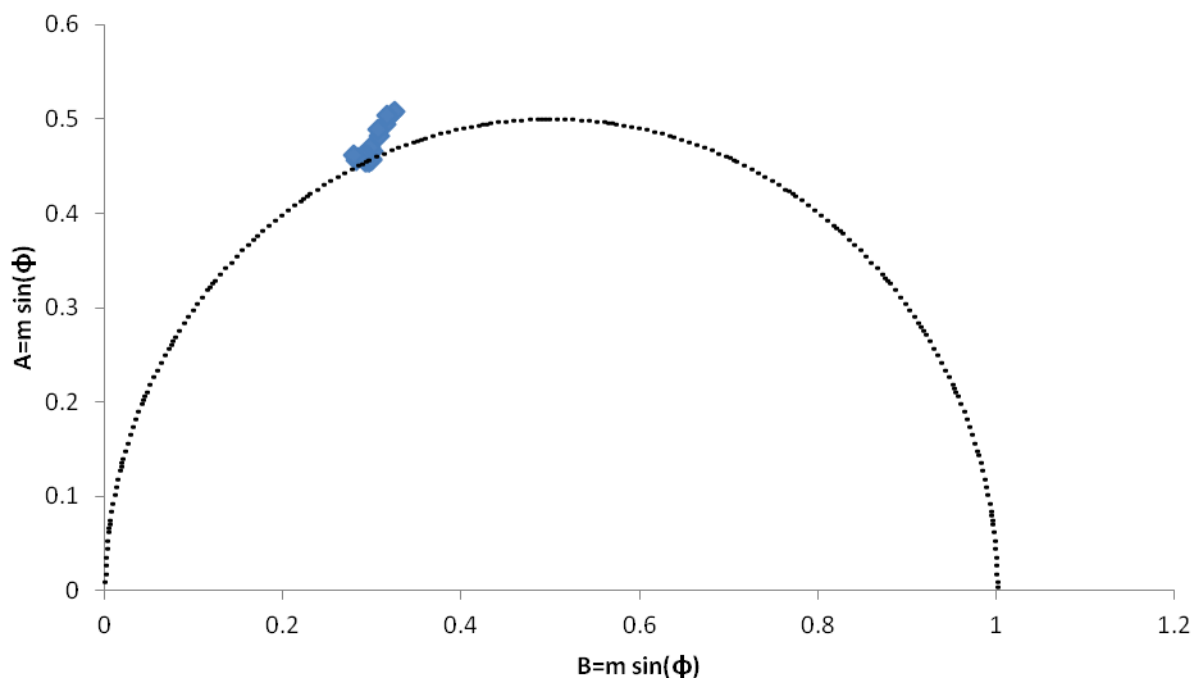


Figure 10: AB plot of 10 μ M rhodamine 6G without potassium iodide quencher in the blacked out lab.

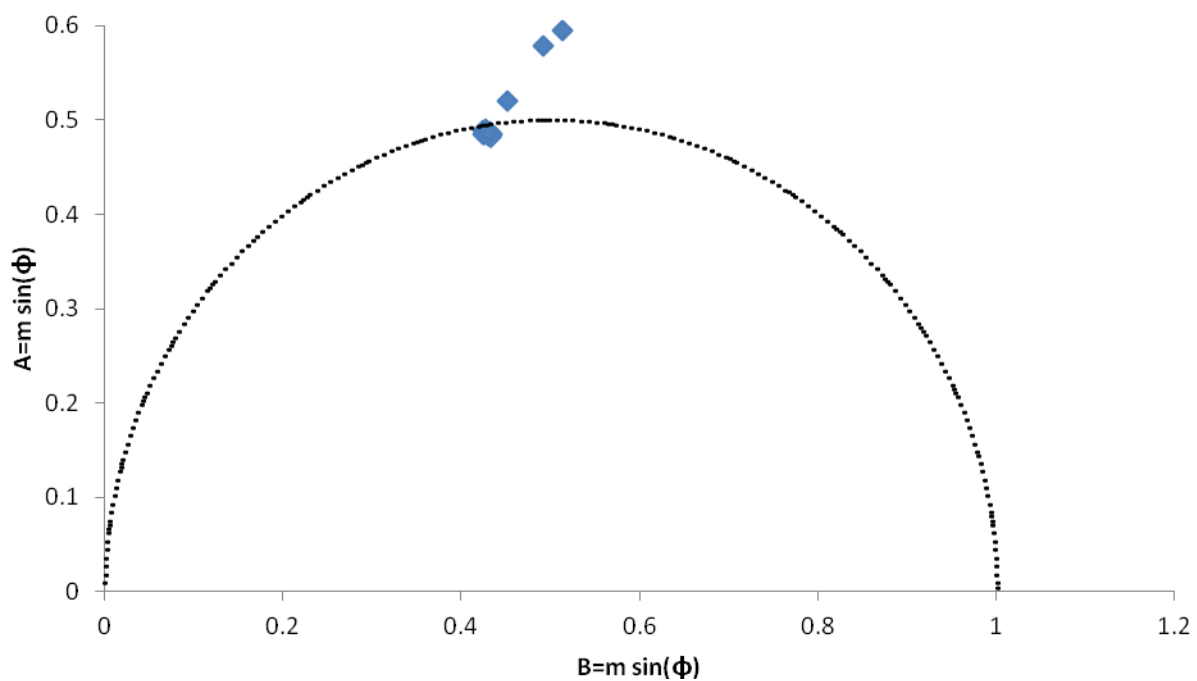


Figure 11: AB plot of 10 μ M rhodamine 6G with 16mM potassium iodide quencher in the blacked out lab.

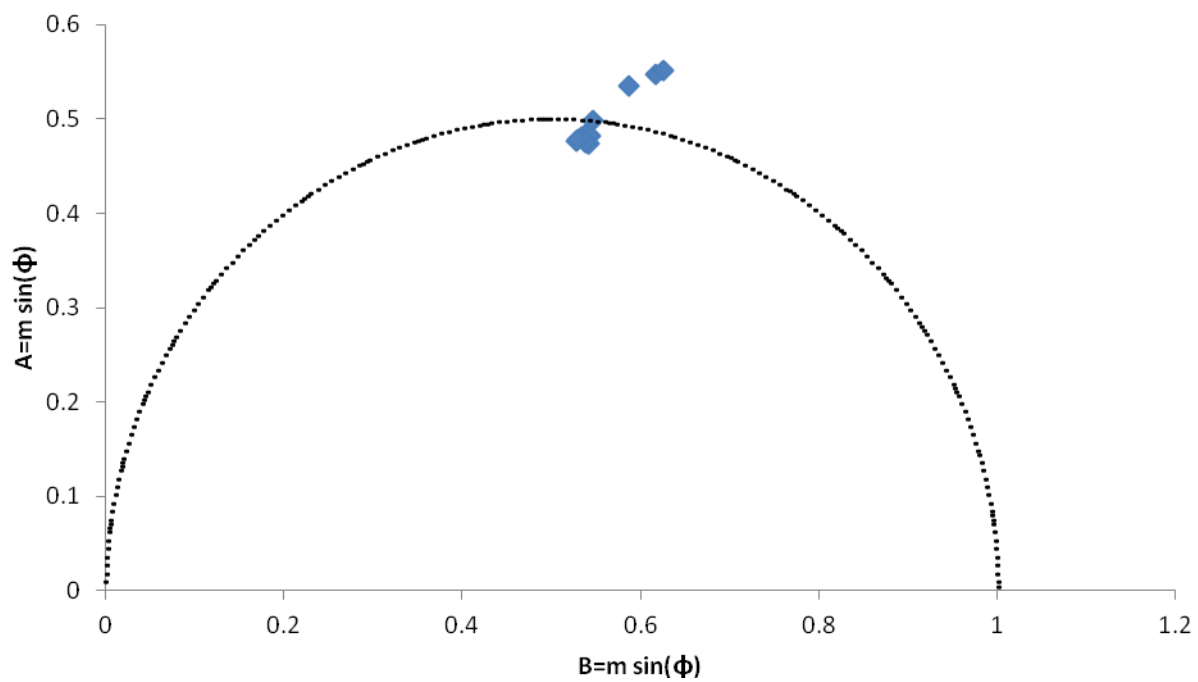


Figure 12: AB plot of 10 μ M rhodamine 6G with 32mM potassium iodide quencher in the blacked out lab.

The data points of Figure 10, Figure 11 and Figure 12 are closely clustered on the one-to-one and track to right.

3.2 Spectra of Fluorophores

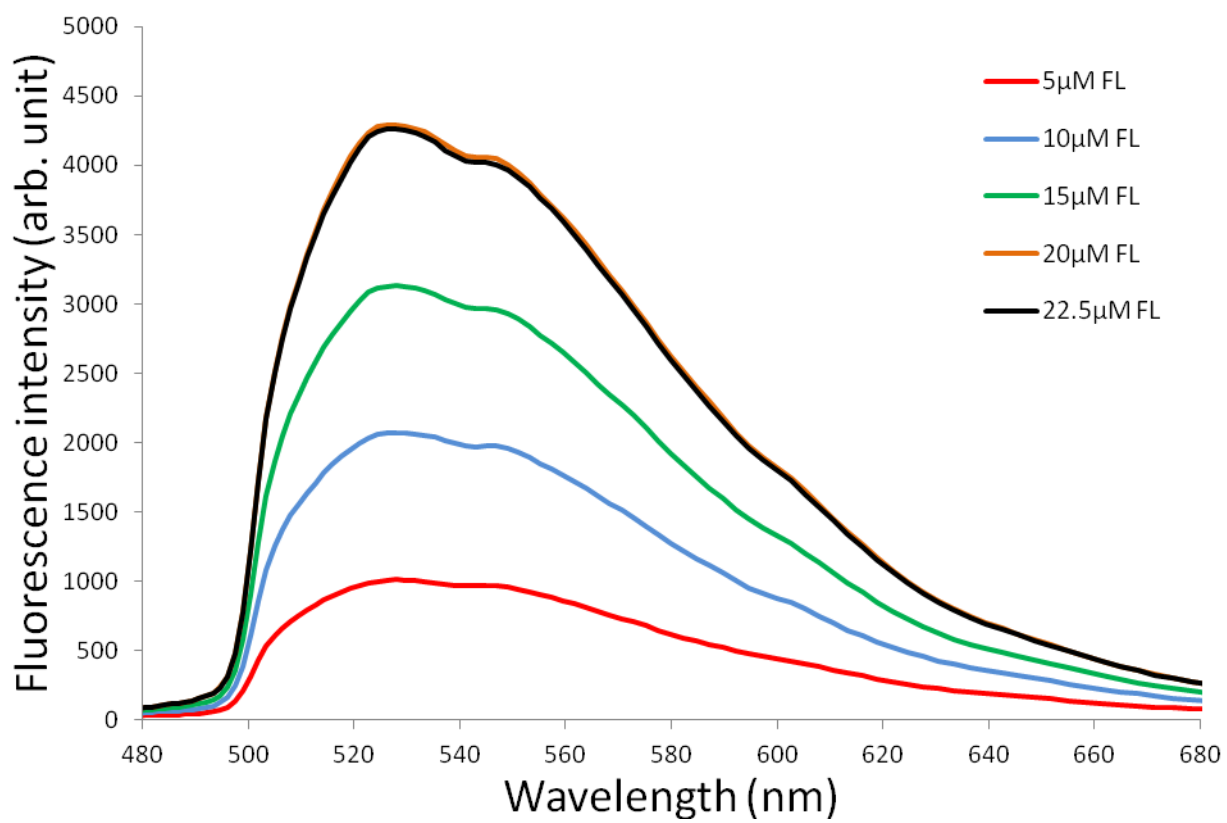


Figure 13: Fluorescein in unbuffered reverse micelles.

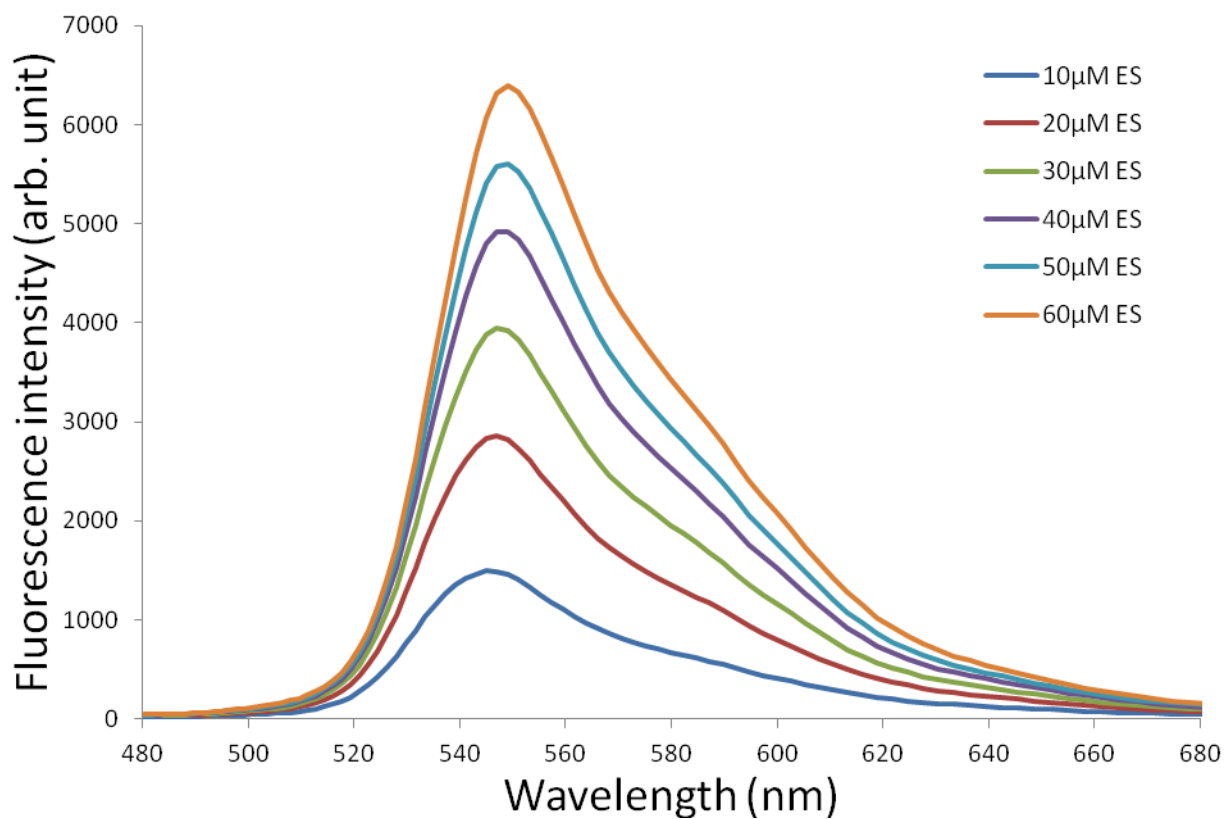


Figure 14: Eosin Y in unbuffered reverse micelles.

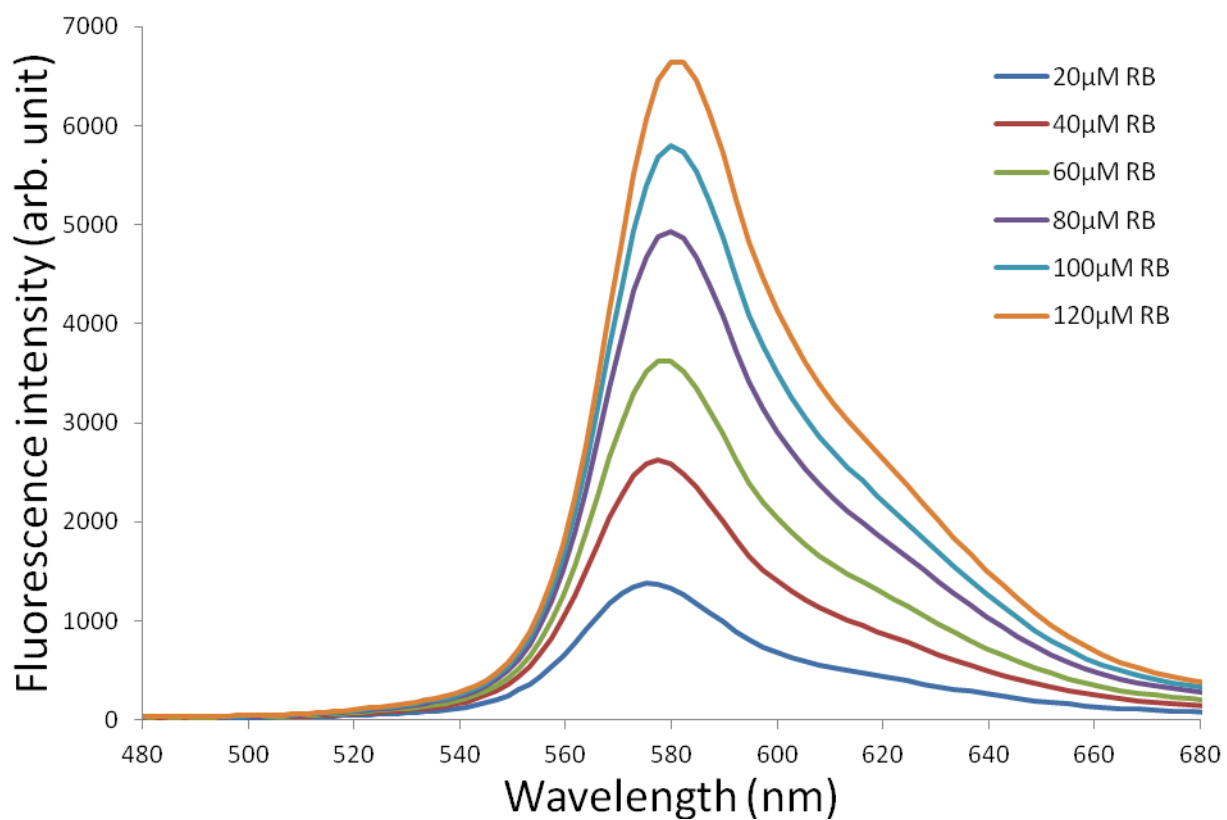


Figure 15: Rhodamine B in unbuffered reverse micelles.

The fluorescence spectra of the fluorophores as seen in Figure 13, Figure 14 and Figure 15 increase with concentration.

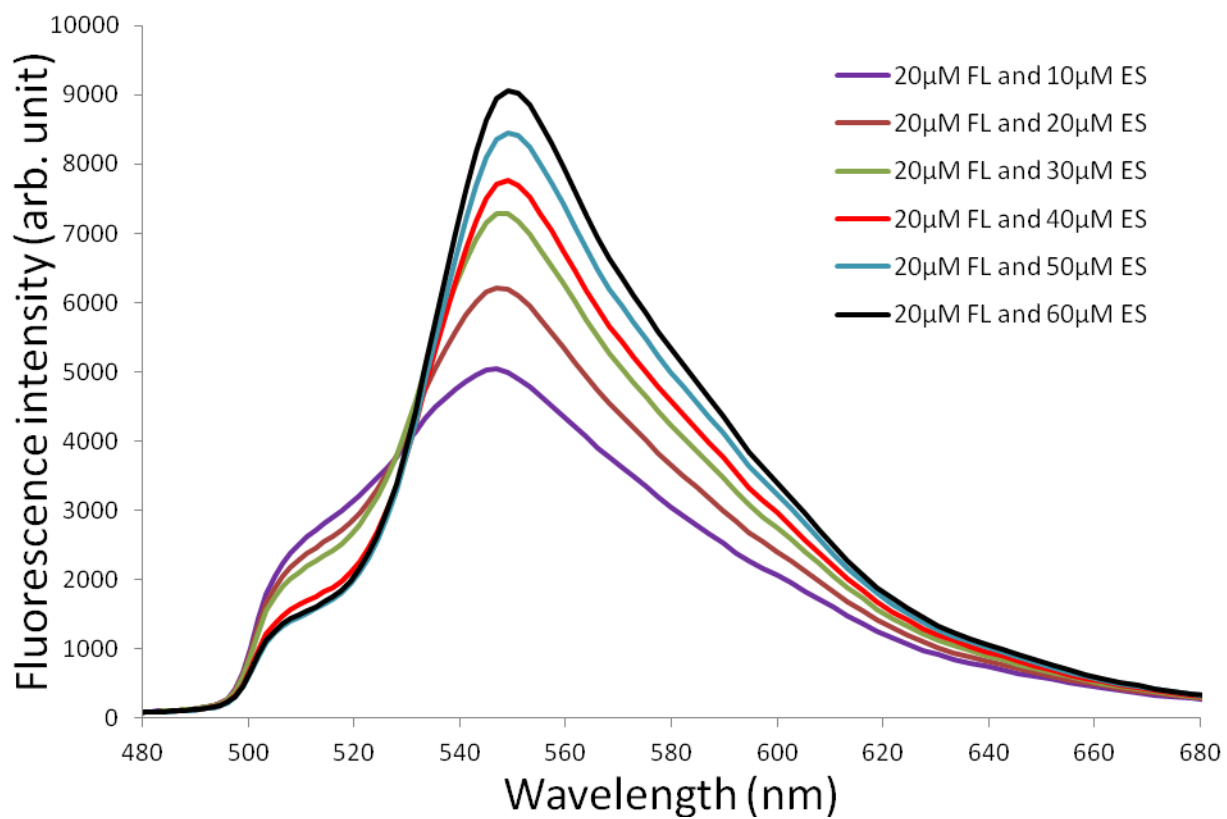


Figure 16: Fluorescein and eosin Y in unbuffered reverse micelles.

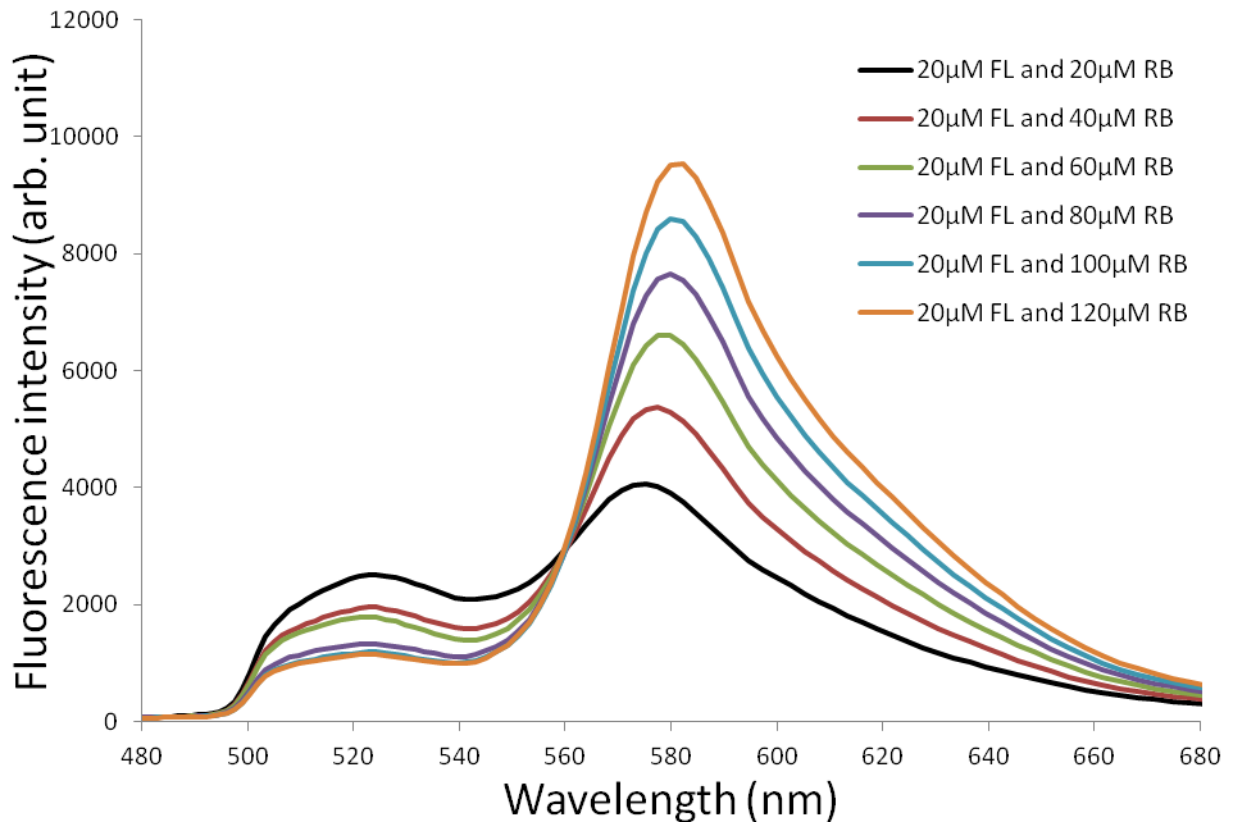


Figure 17: Fluorescein and rhodamine B in unbuffered reverse micelles.

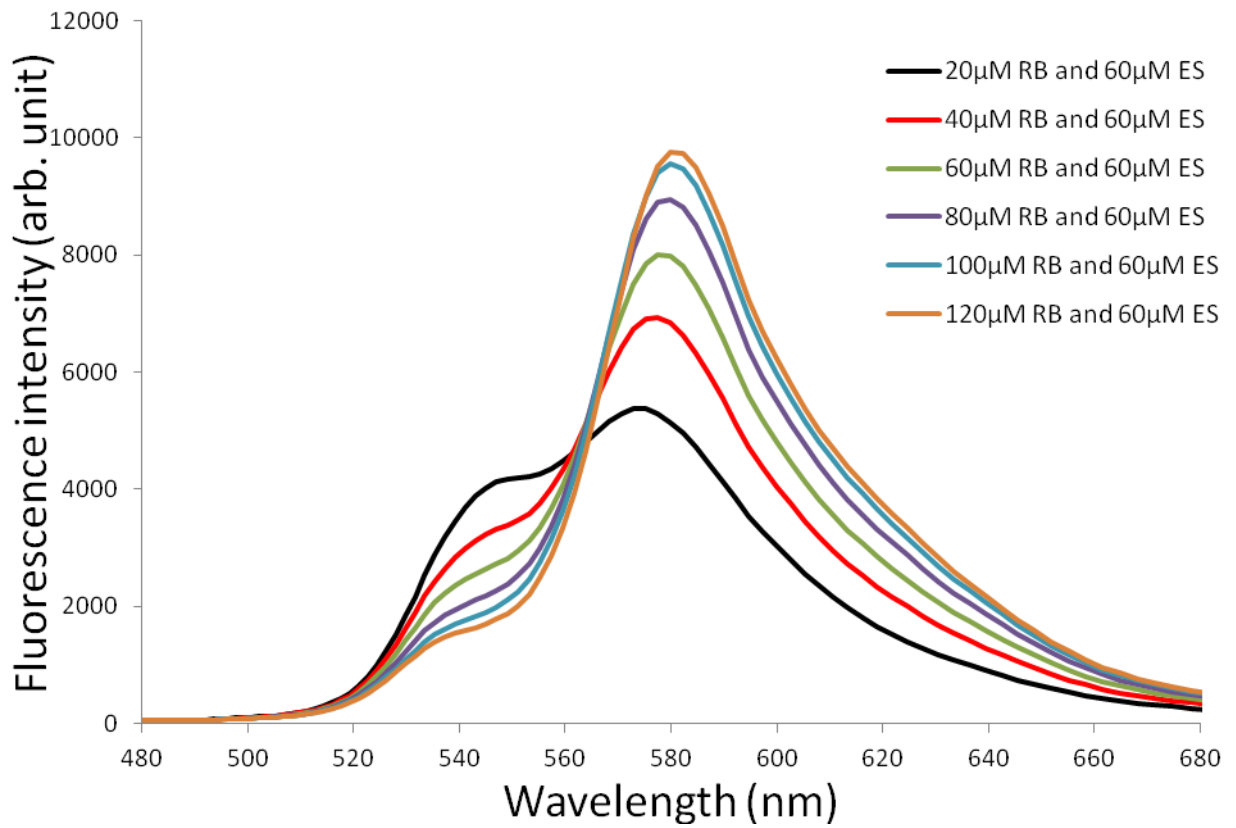


Figure 18: Eosin Y and rhodamine B in unbuffered reverse micelles

In the donor acceptor pairs (Figure 16, Figure 17 and Figure 18) the donor's fluorescence intensity decreases as the acceptors concentration and fluorescence intensity increases.

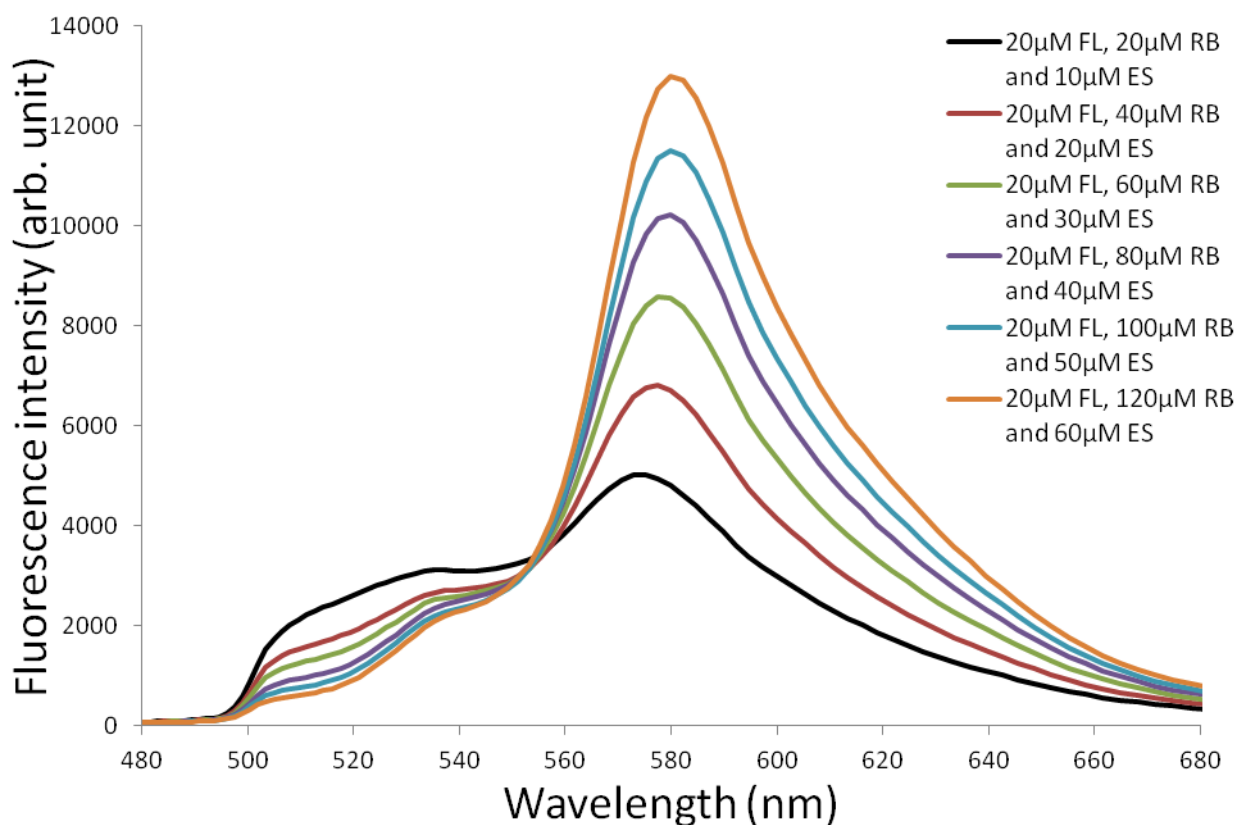


Figure 19: Fluorescein, Eosin Y (ES) and Rhodamine B (RB) in unbuffered reverse micelles.

In a mixture of all three fluorophores (Figure 19) the fluorescence intensity of the terminal acceptor rhodamine B increases, the intensity of both of the other dyes decreases.

3.3 FRET Efficiencies

λ	Donor	Acceptor	Concentration of Acceptor (M)	FRET Efficiency suggested by	
				intensity	Phase lifetime
523	Fluorescein	Eosin Y	0.00000	0.00	0.00
523	Fluorescein	Eosin Y	0.00001	0.11	0.00
523	Fluorescein	Eosin Y	0.00002	0.14	0.00
523	Fluorescein	Eosin Y	0.00003	0.17	-0.11
523	Fluorescein	Eosin Y	0.00004	0.20	-0.02
523	Fluorescein	Eosin Y	0.00005	0.22	0.01
523	Fluorescein	Eosin Y	0.00006	0.24	0.00
523	Fluorescein	Rhodamine B	0.00000	0.00	0.00
523	Fluorescein	Rhodamine B	0.00002	0.34	0.08
523	Fluorescein	Rhodamine B	0.00004	0.47	0.02
523	Fluorescein	Rhodamine B	0.00006	0.56	0.01
523	Fluorescein	Rhodamine B	0.00008	0.65	0.01
523	Fluorescein	Rhodamine B	0.00010	0.70	0.10
523	Fluorescein	Rhodamine B	0.00012	0.72	0.12
543	Eosin Y	Rhodamine B	0.00000	0.00	0.00
543	Eosin Y	Rhodamine B	0.00002	0.31	-0.07
543	Eosin Y	Rhodamine B	0.00004	0.39	-0.10
543	Eosin Y	Rhodamine B	0.00006	0.42	-0.11
543	Eosin Y	Rhodamine B	0.00008	0.44	-0.19
543	Eosin Y	Rhodamine B	0.00010	0.44	-0.19
543	Eosin Y	Rhodamine B	0.00012	0.44	-0.19

Table 1: Intensity and phase lifetimes FRET efficiency from the buffered system.

λ	Donor	Acceptor	Concentration of Acceptor (M)	FRET Efficiency suggested by	
				Intensity	Phase lifetime
523	Fluorescein	Eosin Y	0.00000	0.00	0.00
523	Fluorescein	Eosin Y	0.00001	0.26	0.11
523	Fluorescein	Eosin Y	0.00002	0.36	0.12
523	Fluorescein	Eosin Y	0.00003	0.43	0.22
523	Fluorescein	Eosin Y	0.00004	0.60	0.07
523	Fluorescein	Eosin Y	0.00005	0.66	0.12
523	Fluorescein	Eosin Y	0.00006	0.66	0.21
523	Fluorescein	Rhodamine B	0.00000	0.00	0.00
523	Fluorescein	Rhodamine B	0.00002	0.46	0.05
523	Fluorescein	Rhodamine B	0.00004	0.60	0.00
523	Fluorescein	Rhodamine B	0.00006	0.66	0.03
523	Fluorescein	Rhodamine B	0.00008	0.75	0.03
523	Fluorescein	Rhodamine B	0.00010	0.79	0.07
523	Fluorescein	Rhodamine B	0.00012	0.80	0.17
543	Eosin Y	Rhodamine B	0.00000	0.00	0.00
543	Eosin Y	Rhodamine B	0.00002	0.42	0.10
543	Eosin Y	Rhodamine B	0.00004	0.57	0.06
543	Eosin Y	Rhodamine B	0.00006	0.67	0.00
543	Eosin Y	Rhodamine B	0.00008	0.74	0.10
543	Eosin Y	Rhodamine B	0.00010	0.79	0.05
543	Eosin Y	Rhodamine B	0.00012	0.82	0.12

Table 2: Intensity and phase lifetimes FRET efficiency from the un-buffered system.

In Table 1 and Table 2 there is a clear lack of correlation between the FRET efficiency suggested by intensity and the FRET efficiency suggested by the phase lifetime.

3.4 Cell Work

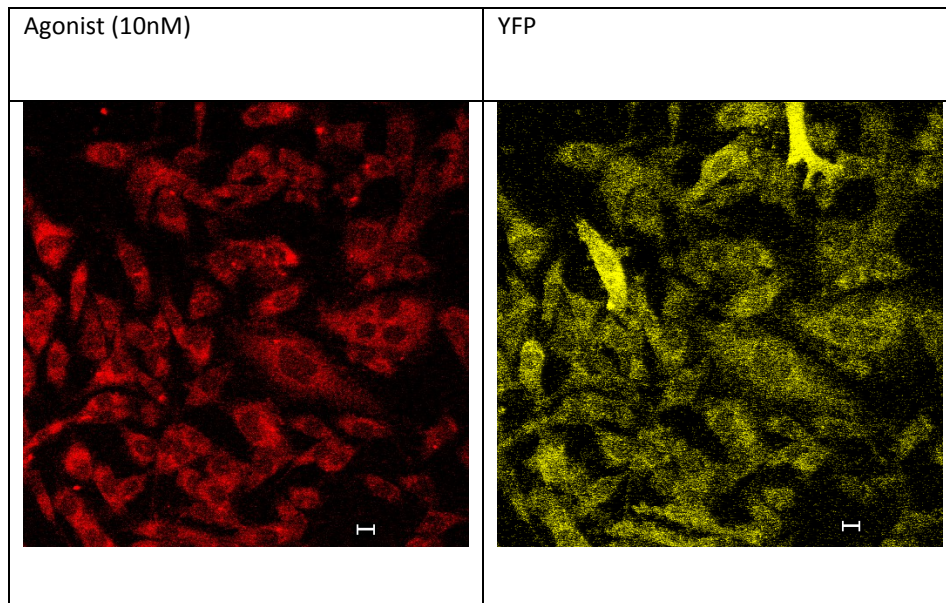


Figure 20: Fluorescent agonist and YFP imaged on the confocal microscope (Scale Bars 10 μ M).

Figure 20 and Figure 21 show colocalisation of YFP and the CellAura agonist, with an overlap

Coefficient: $r=0.783$

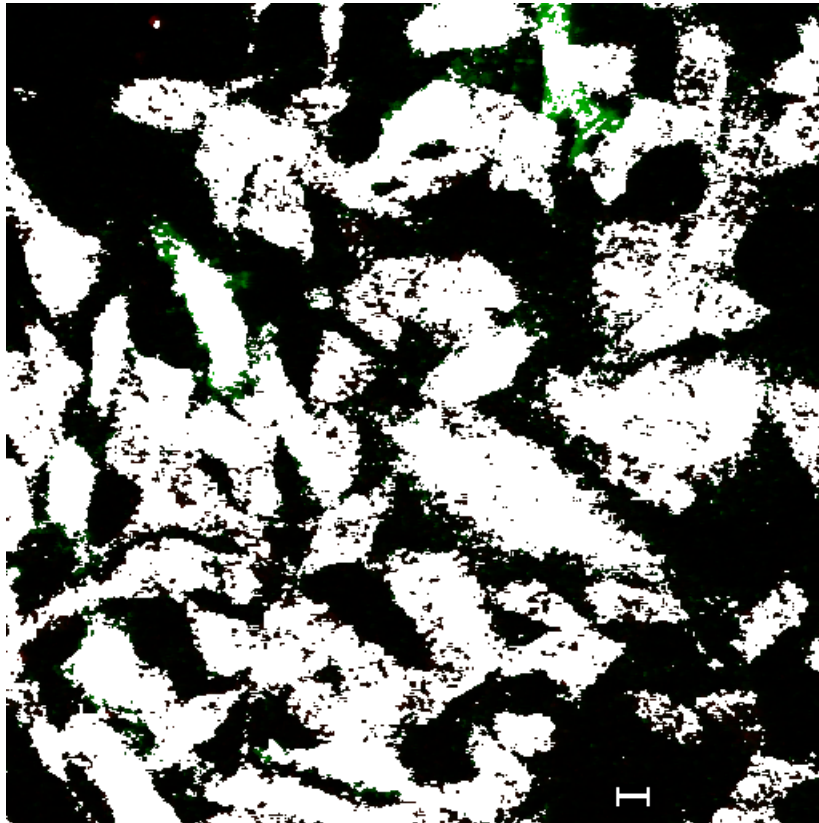


Figure 21: Costes' Mask for the YFP and agonist incubated without DPCPX, white areas represent colocalisation, green areas have agonist or YFP but not both and black areas have neither (Scale Bar 10 μ M).

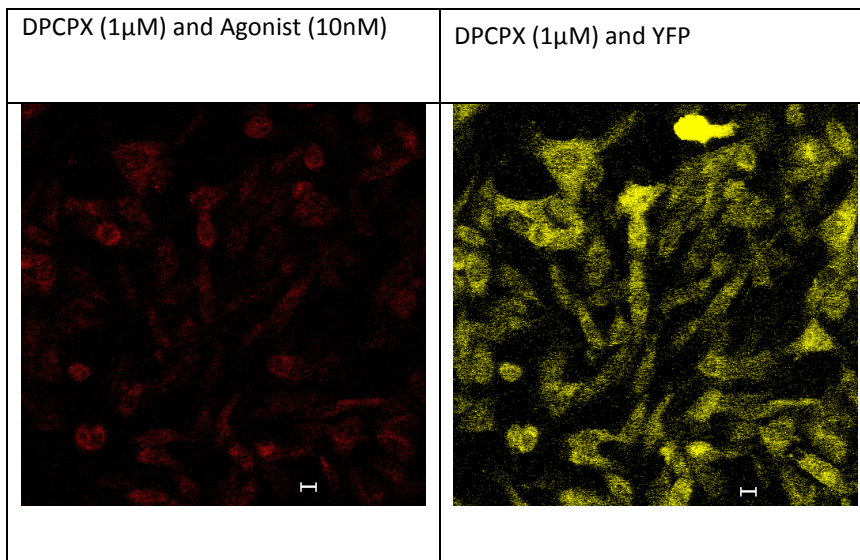


Figure 22: Fluorescent agonist and YFP imaged in the presence of DPCPX on the confocal microscope (Scale Bars 10 μ M).

Figure 22 and Figure 23 show colocalisation of YFP and the CellAura agonist in the presence of DPCPX, with an overlap Coefficient: $r=0.711$.

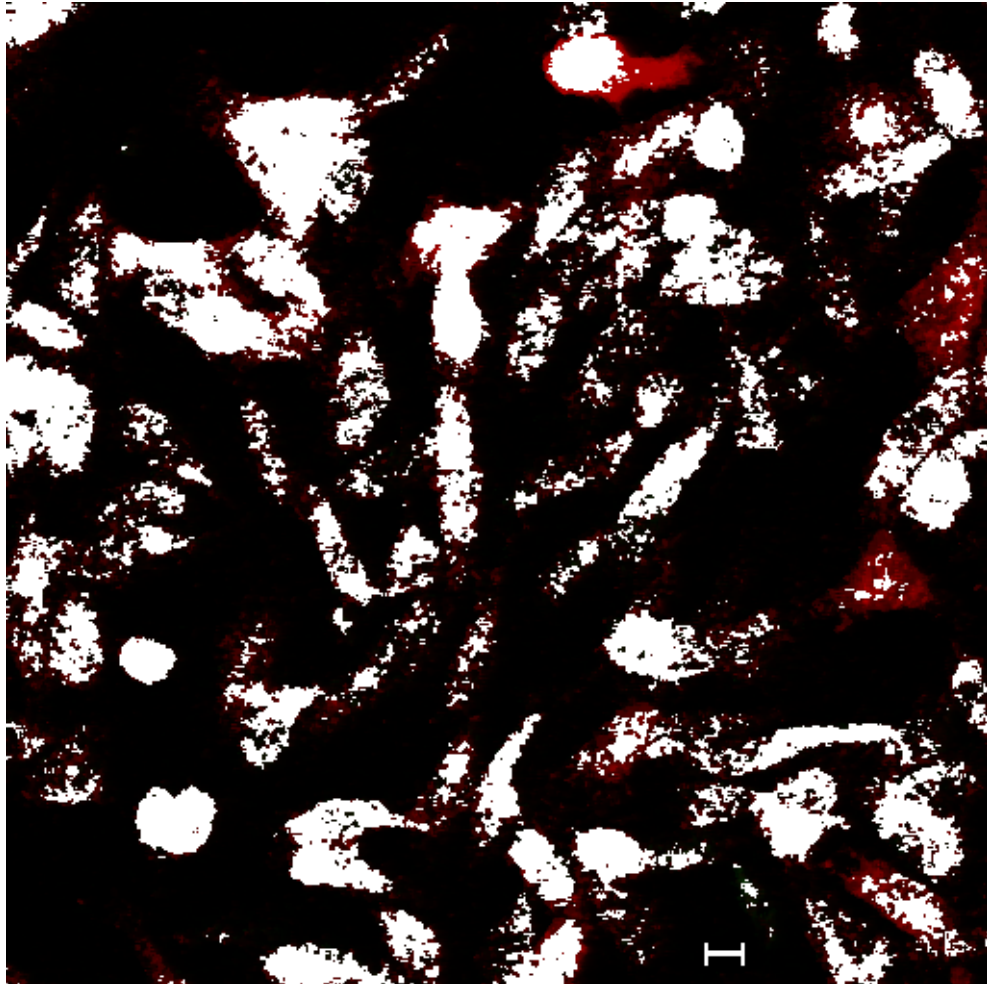


Figure 23: Costes' Mask for the YFP and agonist incubated with DPCPX, white areas represent colocalisation, red areas have agonist or YFP but not both and black areas have neither (Scale Bar $10\mu\text{M}$).

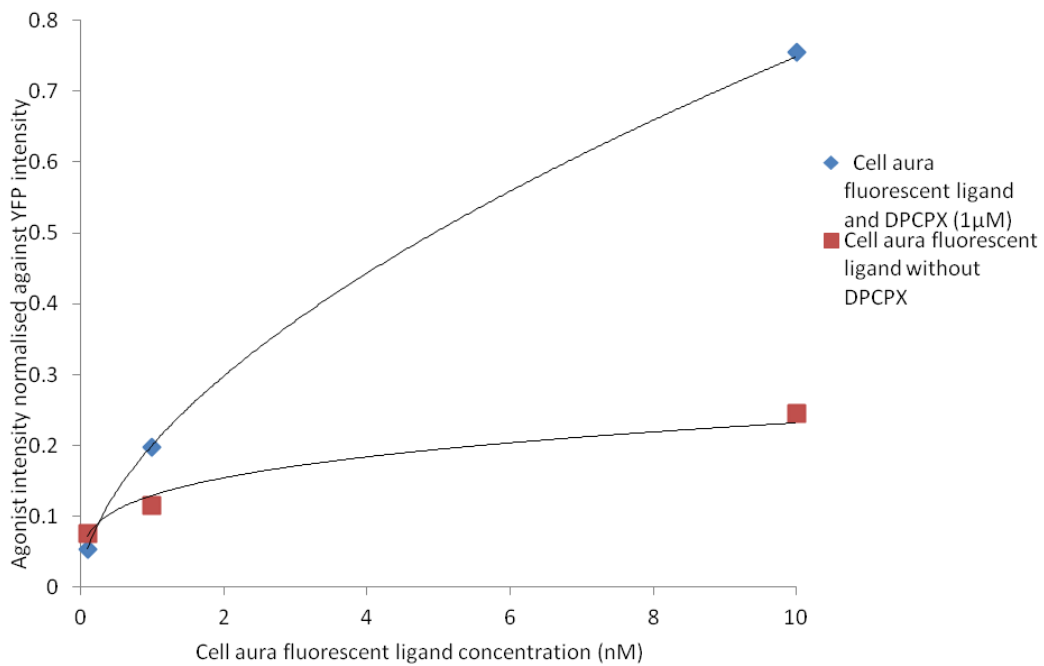


Figure 24: Log plot of agonist intensity normalised against YFP.

In Figure 24 it is demonstrated that at higher concentrations of the agonist, the reduction in fluorescence seen with DPCPX is more pronounced.

3.5 Anisotropy

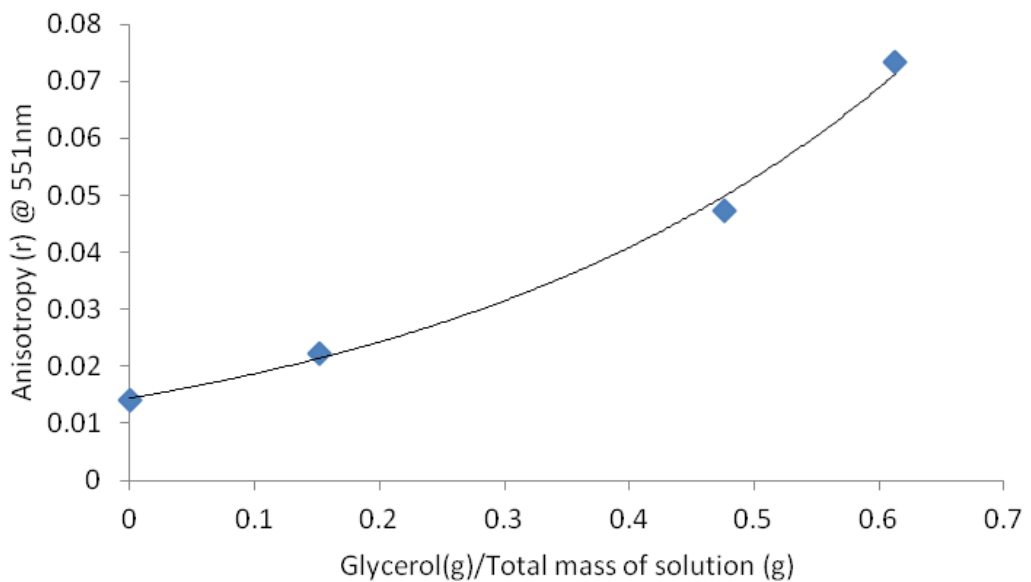


Figure 25: Anisotropy of rhodamine 6G in glycerol and water.

In Figure 25 the anisotropy of the rhodamine 6G increases as the proportion of glycerol solution increases.

Discussion

4.1 Initial Data

Initial measurements using our microscope system were unable to produce lifetimes. Binary mixtures of dyes in water and in SDS micelles, reverse micelles, different concentrations of fluorescein in SDS, different concentrations of SDS with rhodamine 6G and buffered dye mixtures were investigated. These experiments provided good spectral data.

We then attempted to look at the lifetimes with the spectral data. To aid this we switched to nunc glass bottomed plates from Costar 3603 plastic bottomed plates. These have been found by our group to produce less auto-fluorescence, reducing the potential noise in our lifetime measurements.

The effects of the concentration on rhodamine 6G, Fluorescein quenching, iso-octane reverse micelles, were imaged with lifetimes and intensities. These still showed evidence of noise although its origins were not obvious; possible culprits appeared to be external light sources or the zeroing system of the machine.

Experiments with R6G being quenched with potassium iodide initially shows classic quenching behaviour with a lifetime shortening as the concentration of quencher increases. However, over a certain concentration AB plots of the data shows the cluster of lifetimes moving off the one to one semicircle into the semicircle (see *Figure 7, Figure 8 and Figure 9*). A noise source was suspected as the cause of this behaviour.

Noise from the plastic plates had already been reduced through the introduction of the glass bottomed nunc plates. In an attempt to reduce noise due to light from sources not connected to the microscope both inside and outside the lab windows were covered with an opaque material. Light sources within the lab including power sockets LEDs on computer equipment screens and displays were all covered unless essential to the experiments being performed. The eyepieces of the microscope were also covered to prevent the collection of ambient light into the microscope. The 96 well plates used for imaging were fitted with opaque lids to further reduce light entering the microscope from sources other than sample.

The rhodamine 6G quenching experiment was repeated this time with the background light elimination measures in place and it showed much clearer tracking of the phase modulation one-to-one line on AB plots (see Figure 10, Figure 11 and Figure 12) suggesting a substantial reduction of the background noise.

A repeat of the rhodamine 6G quenching experiment although this time with constant ionic strength showed slight deviation from the one-to-one modulation and phase line on an AB plot. Although this may have been due to the maintenance of a constant ionic strength these deviations were more likely due to safety policy requiring a small square of lab window to be left uncovered, this was implemented between the running of these experiments, a removable shield was used to cover this area during experiments leading to a small amount of light still being able to enter the lab.

Anisotropy was looked at in a simple Rhodamine 6G, water and glycerol mixture. The anisotropy value (r) for the solutions increased as the ratio of glycerol to water increased. This is expected due to the slowed rotation of the fluorophore reducing the amount of depolarisation observed. Although slightly lower, our values are comparable to those of the literature (they give an r value of 0.07 -0.09 for a 50% glycerol solution(Zhou et al., 2009), our 60% solution only gave an r of 0.07) (see

Figure 25). This may require a revision of our G factor (A factor calculated to deal with any unavoidable misalignment of the polarisers).

4.2 Cell work

The sequencing data from the plasmids shows that the constructs contain both the adenosine A₁ receptor and the YFP/CFP sequences. The confocal microscope has been used to image our cells with the CellAura 633 AG fluorescent agonist. These experiments have been carried out on cells with and without pre-treatment with DPCPX to look at non-specific and specific binding (Figure 20 and Figure 22). The agonist intensities were normalised against YFP emission. Cells incubated with DPCPX and agonist show a reduction in fluorescence intensity due to the fluorescent ligand being prevented from binding to the A₁R, compared to cells incubated only with ligand and therefore specific binding is occurring however there is still a signal from the ligand which is co-localised to the cells this suggests non-specific binding as does the overlap Coefficients are well under 1($r=0.711$ with DPCPX and $r=783$

without DPCPX) the CellAura data sheet suggests that the agonist will also bind to the adenosine A_{2A} and A₃ receptors thus this is likely what we are seeing. At concentrations of agonist above the 1.00×10^{-8} M the level of non-specific binding is less than 16% of the total binding (Figure 24).

4.3 Moving on to the model system

Our experiments characterising the lifetime of eosin Y solutions made up using the disodium salt had a lifetime of 1.1 ns and lay on the one-to-one phase modulation line of an AB plot. As a result we could be confident that the lifetimes were getting were reasonably accurate and useful given that the literature found eosin Y was 1.18 ± 0.05 ns. (Wyatt et al., 1987)

Using the Jiang paper as a guide we looked at rhodamine B, eosin Y and fluorescein, buffered at pH 9.6 and unbuffered in reverse micelles of AOT, isooctane and water. Their concentrations were adjusted until their intensities were comparable. The spectra were good (Figure 13, Figure 14, Figure 15, Figure 16, Figure 17, Figure 18 and Figure 19). Rhodamine B and eosin Y mixtures seemed to show some linear mixing with no evidence of FRET, rhodamine B and fluorescein as well as eosin Y and fluorescein appeared to show linear mixing although not as clearly as that in the rhodamine B and eosin Y mixture on an AB plot. The only part of the rhodamine B and eosin Y mixture which shows a clear line linking the values expected is the lone eosin Y, rhodamine B. However, in the rhodamine B and fluorescein mixture as with the eosin Y and fluorescein mixture the line only links to fluorescein; it tracks in the direction of the other fluorophore and does not reach them. This may suggest a complex of fluorescein and the other dye exhibiting this midpoint lifetime. The lifetime showed no evidence of FRET in the systems. The results of the experiment interestingly seemed to show low noise and a possible reason for this was the matching of the intensities of the dyes and the standard.

The microscope system has software for both acquisition and image processing; the image processing side requires a sample of fluorophore with a known lifetime to be used as a standard and from this can calculate the lifetimes of the samples. It appeared the differences in intensity of samples and standards can affect the ability of the software to use the standard to remove noise from the measured lifetimes. This effect is particularly obvious if the auto expose option is utilised.

To test this data, the quenching of rhodamine 6G with potassium iodide was plotted as a Stern-Volmer plot and then compared to the literature, matching the intensities and turning off auto expose improved the similarity of our experiments and data to those in the literature.

4.4 No FRET

Confident now that the microscope system produced good lifetime data, the Jiang paper was repeated with buffered dye solutions. Using this data we calculated FRET efficiency (E) suggested by intensity changes using the unmixed spectra (I_{da}) and data for the fluorophores alone at the same concentration (I_d) in Equation 8 and by the phase lifetime at the peak intensity of the donor with acceptor τ_{da} and without τ_d using Equation 9.

Equation 8:

$$E = 1 - \frac{I_{da}}{I_d}$$

Equation 9:

$$E = 1 - \frac{\tau_{da}}{\tau_d}$$

These showed large amounts of FRET when looking at the intensity data (FRET efficiency values are the fraction of donors which transfer energy to an acceptor through FRET, a value of 1 would be 100% of the donors undergoing FRET, 0.5 would be 50% and 0 would be 0%) but no signs of the extensive FRET suggested by the paper are seen in the lifetime measurements, only small amounts at the highest concentrations (Table 1). This experiment was repeated with unbuffered dyes because it was not clear if the original study buffered the dyes and it was possible that buffering was the cause of the lack of FRET. However it did not seem to increase the level of FRET in the system; which again showed large amounts of FRET when looking at intensities, but little evidence of FRET using the

lifetime data (Table 2). One difference seen in all of the dye combinations was a reduced intensity FRET value when unbuffered; this suggests that the donor dyes are being affected by pH changes in the unbuffered solutions possibly by conversion to one of their species to another with a different absorbance and emission spectrum. These changes appear to enhance the intensity decreases seen in the donor dyes in the unbuffered systems. Plotted as graphs: Figure 26,

Figure 27 and Figure 28, it is obvious the amount of FRET suggested by the intensities is not reflected in the lifetime data in either the buffered or unbuffered system.

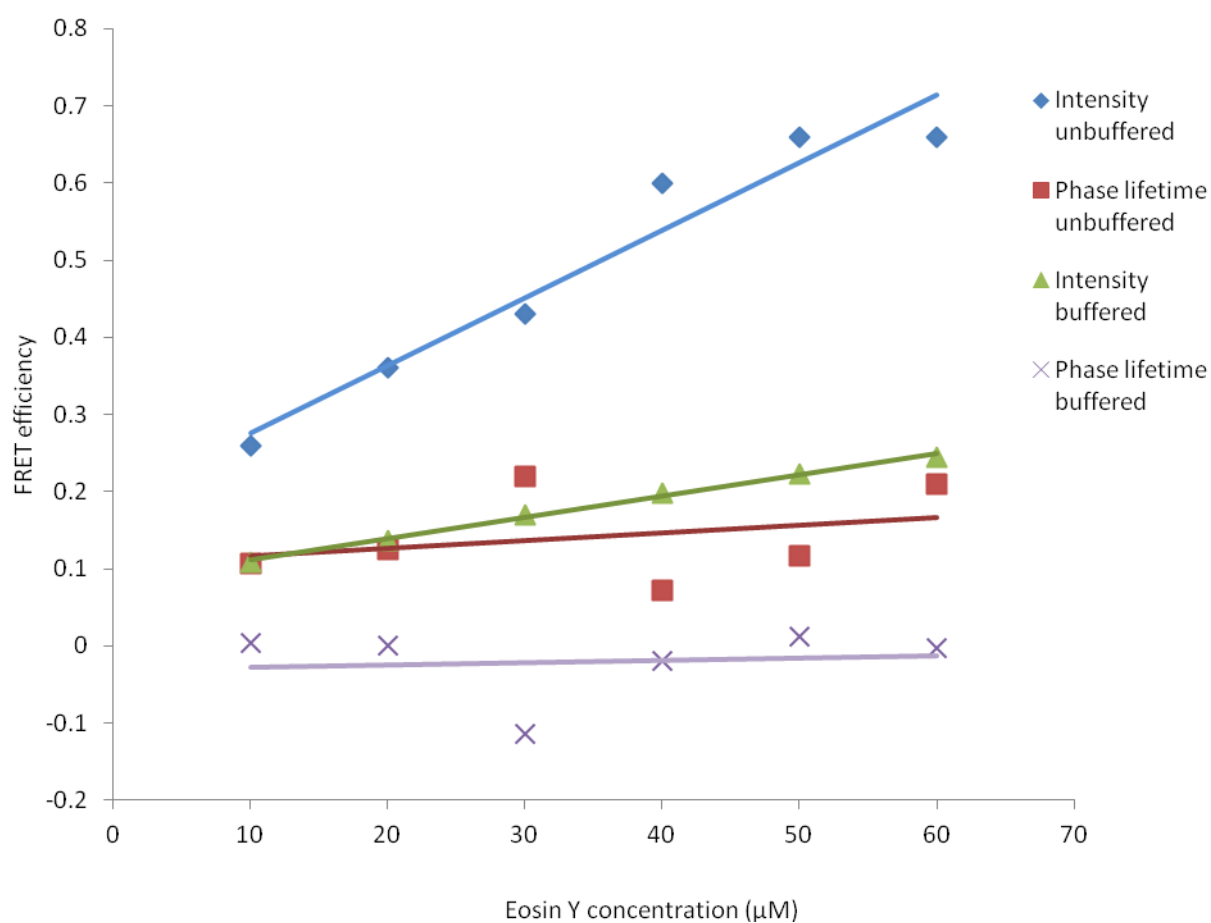


Figure 26: FRET efficiency between FL (20µM in all cases) and ES, calculated using phase lifetime and intensity, in buffered and unbuffered AOT micelles.

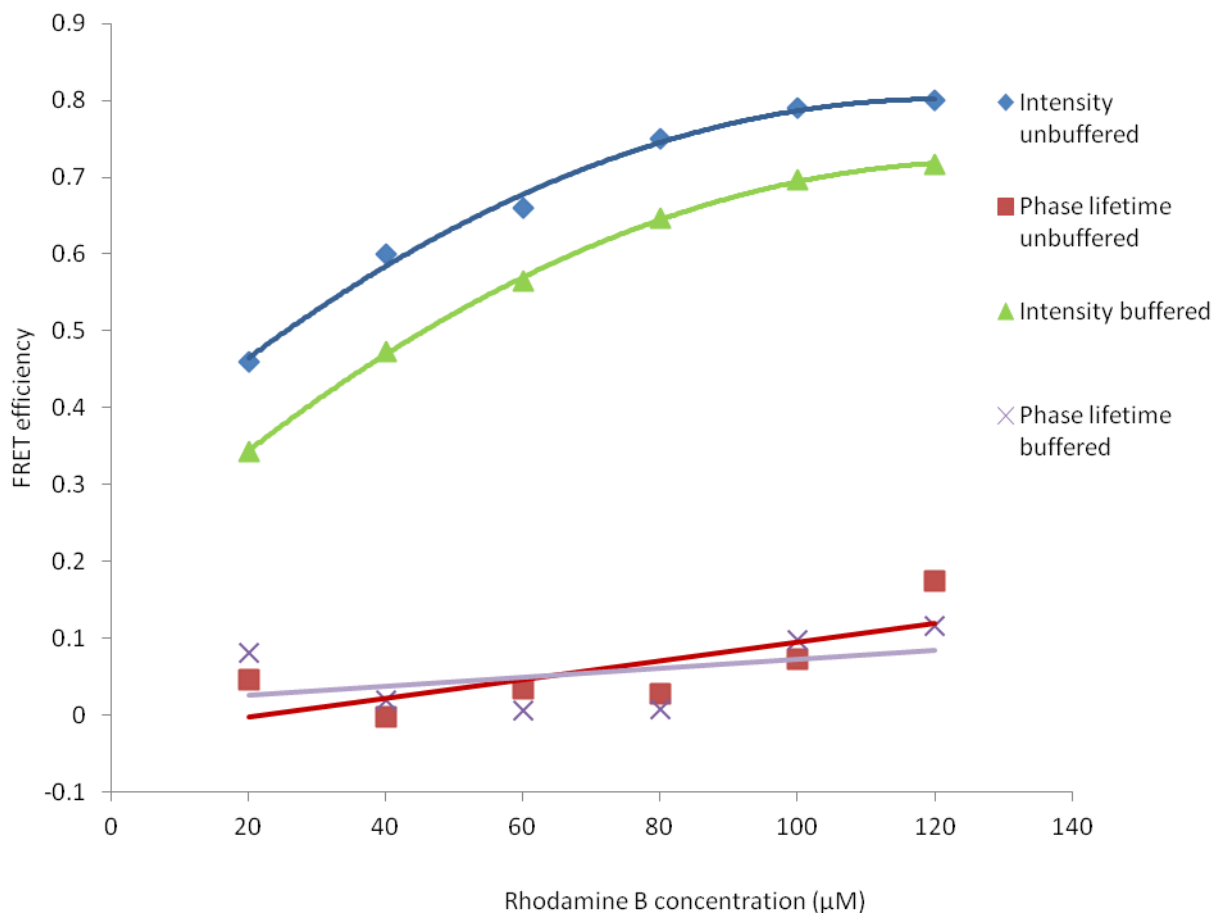


Figure 27: FRET efficiency between FL (20 μM in all cases) and RB, calculated using phase lifetime and intensity, in buffered and unbuffered AOT micelles.

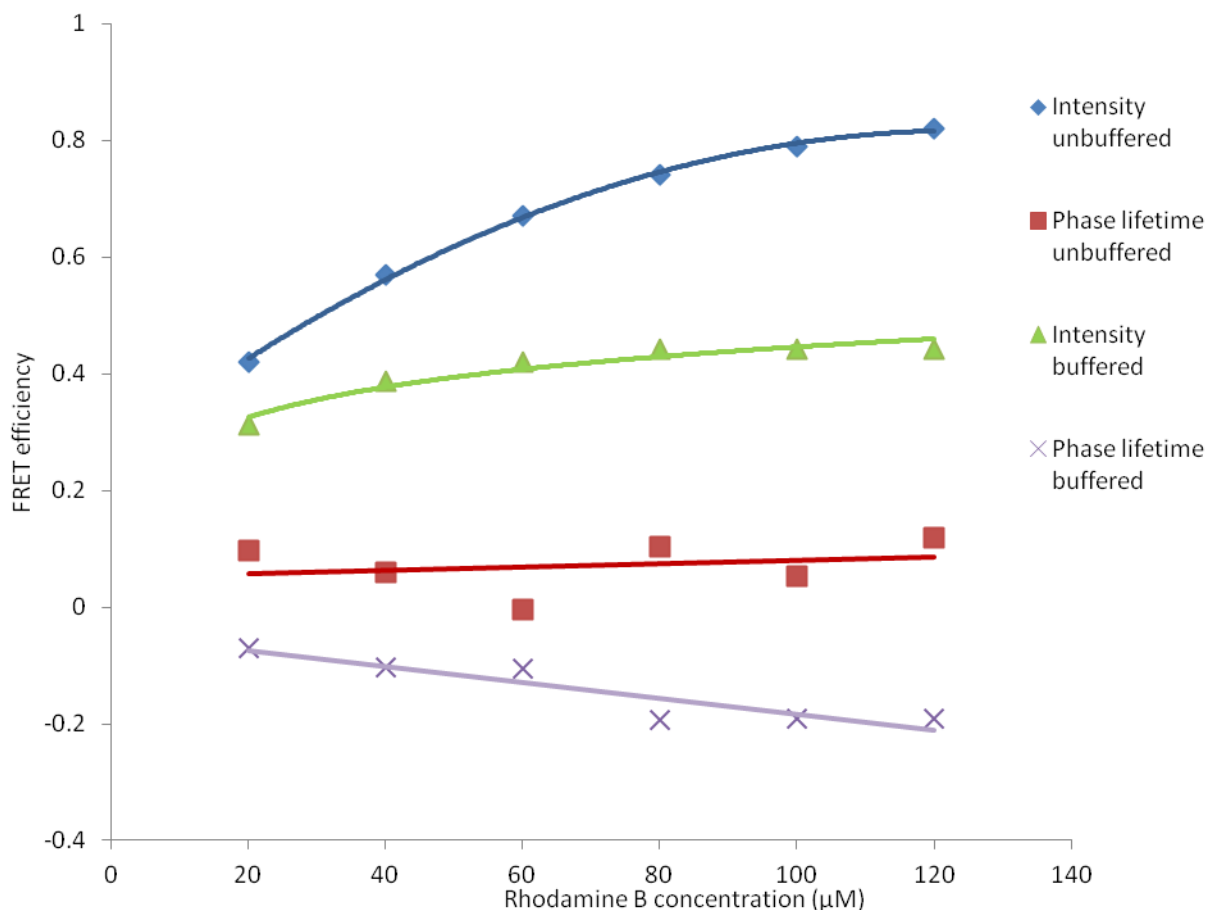


Figure 28: FRET efficiency between ES (20 μM in all cases) and RB, calculated using phase lifetime and intensity, in buffered and unbuffered AOT micelles.

Looking at the intensity data alone for each of the pairs, it would be concluded that there is very high FRET efficiency. However the phase lifetime data suggests little to no FRET. The Jiang paper having only considered the intensity may have come to the wrong conclusion about the reverse micelles systems level of FRET and thus its suitability as a model system.

4.5 Why No FRET

To try and establish the source of the donor quenching, a Stern-Volmer plot was produced using the unmixed spectra in the unbuffered data (for the rest of the analysis the unbuffered data was used as the Jiang paper didn't appear to have buffered it's dyes). If the quenching of the system is dynamic then a Stern-Volmer plot of lifetime or intensity will produce the same curve. As can be seen in

Figure 29 this is not true in our system. This suggests that the reduction in intensity seen is due to some form of static quenching.

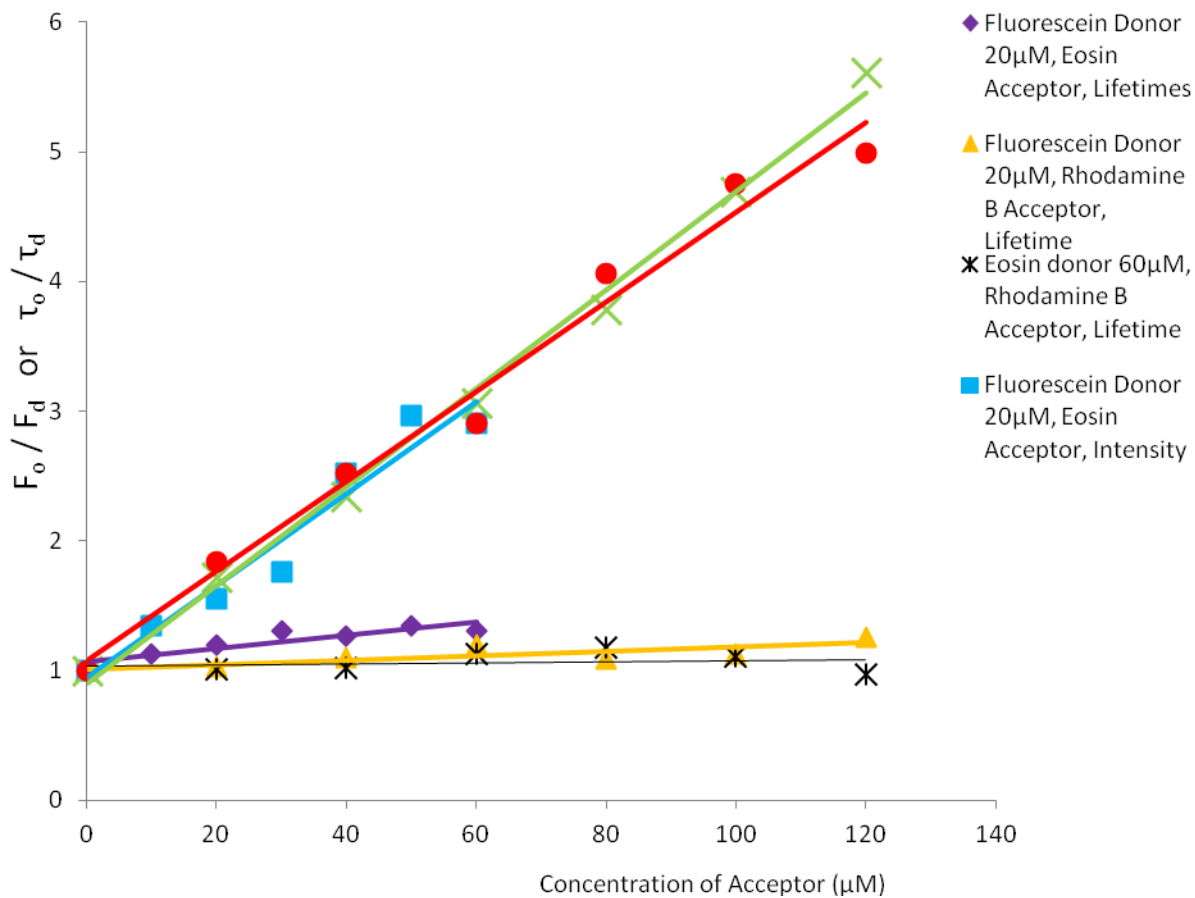


Figure 29: Stern Volmer plot.

The shape of the curve on the Stern-Volmer plot also allows us to determine if static and dynamic quenching is occurring. In a system displaying both static and dynamic quenching the Stern-Volmer plot will curve upwards and in a system with two species being quenched it will curve downwards (Lakowicz, 1999). When the system is displayed as a Stern-Volmer plot it produces a straight line with no discernible curve, suggesting that a single type of quenching is occurring (which we have established to be static quenching due to the lack of lifetime change), and a single species being quenched. (Johansson and Cook, 2003)

At the concentrations used in the Jiang study the solutions are very optically dense this likely leads to inner filter effects. Absorption flattening was also considered as it can produce effects similar to the

inner filter effect however it was found that the micelles are likely too small for this to be significant (Duysens, 1956; Wittung et al., 1994; Abel et al., 2004; Vasquez et al., 2011). The inner filter effects could cause a reduction in intensity like what was seen in the samples causing the façade of FRET. From the absorbance measurements of the single dyes the molar absorptivities were calculated (Figure 30).

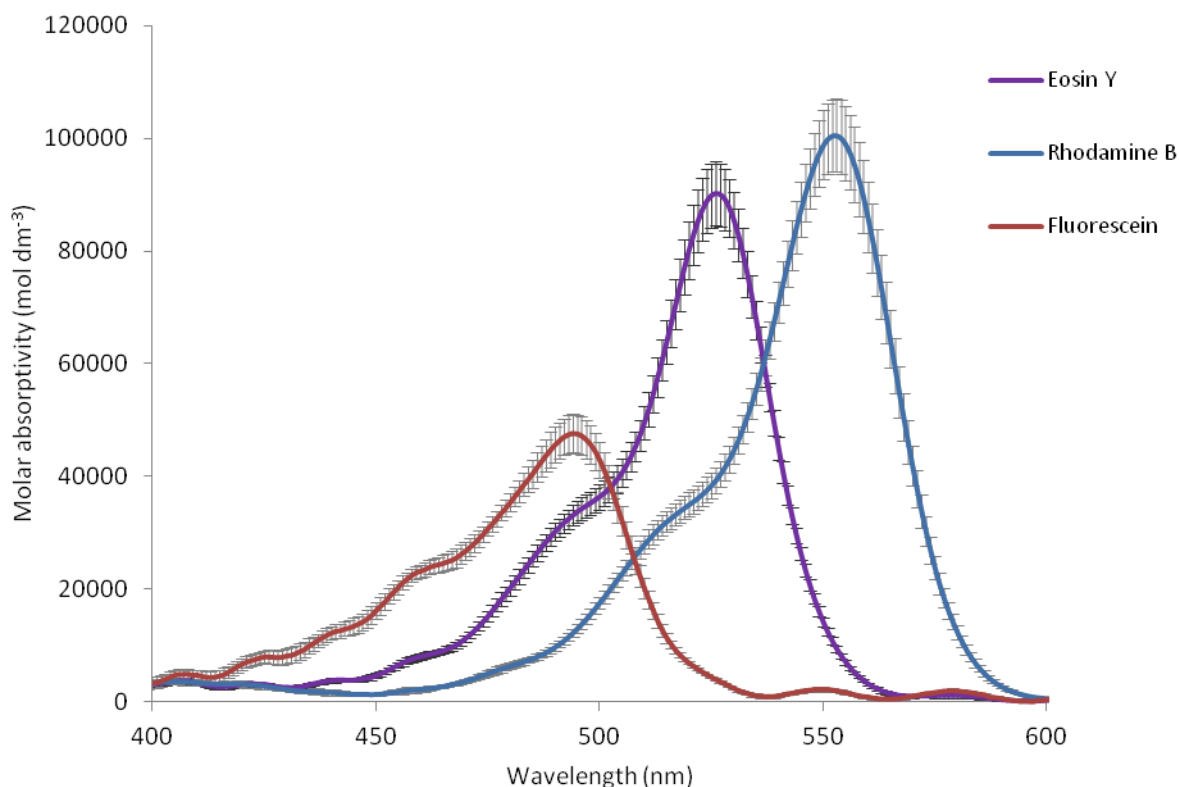


Figure 30: Molar absorptivity of the dyes in reverse micelles (error bars show standard deviation).

The molar absorptivities from the experimental data and the Jiang paper were then used to calculate the levels of FRET expected due to primary inner filter effects (excitation light being absorbed by concentrated solution to the point that the whole sample is not illuminated). Using the molar absorptivities of the donor (ϵ_d) and acceptor (ϵ_a), along with the concentrations of donor (c_d) and acceptor (c_a), Equation 10 can be used assuming sufficient optical density to absorb all light and a homogenous distribution of the fluorophores to calculate the suggested FRET efficiency:

Equation 10:

$$E = \frac{\epsilon_d C_d}{\epsilon_d C_d + \epsilon_a C_a}$$

Figure 31, Figure 32 and Figure 33 show the levels of FRET predicted by the molar absorptivities compared to those calculated from lifetime and intensity data. It was assumed that all the incoming light was being absorbed by the sample and that the different fluorophores would absorb a proportion of the light equal to the ratio of their absorbance at that concentration to the absorbance of the other dye in the solution.

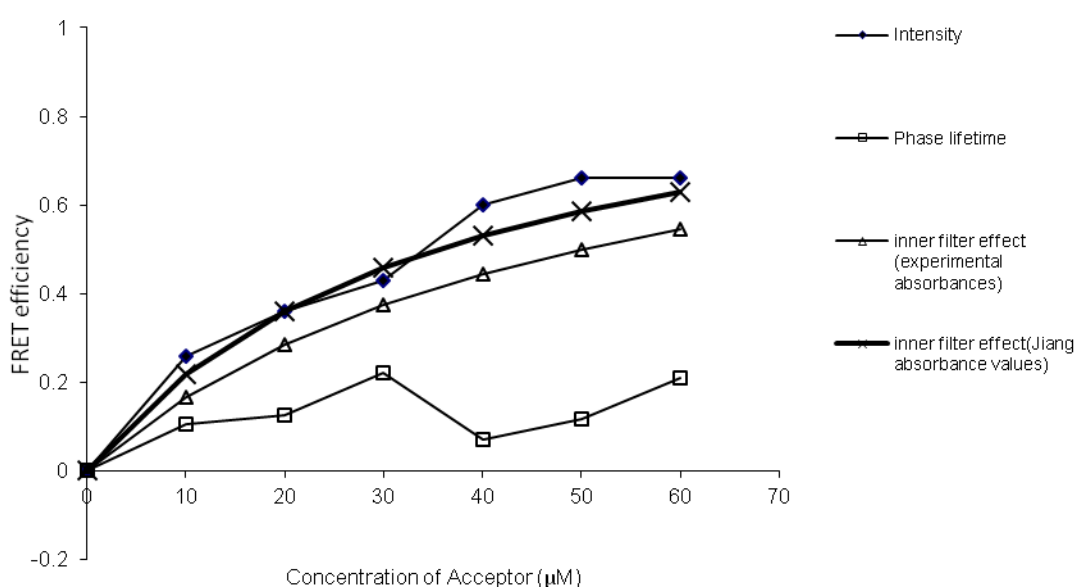


Figure 31: Levels of FRET suggested by different attributes of the system, Fluorescein donor at 20µM, eosin Y as acceptor.

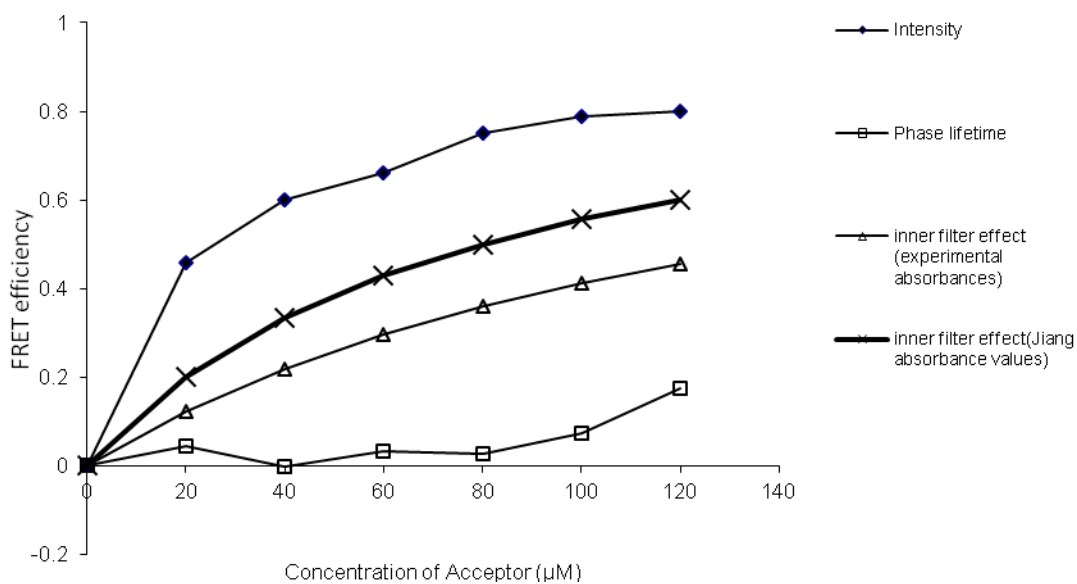


Figure 32: Levels of FRET suggested by different attributes of the system fluorescein as donor at 20 μM , Rhodamine B as acceptor.

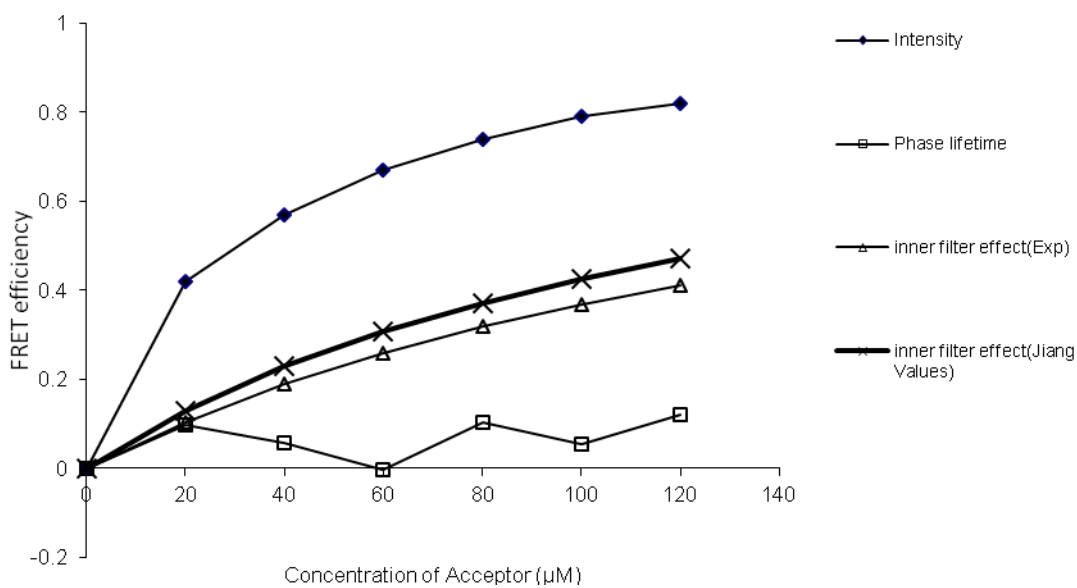


Figure 33: Levels of FRET suggested by different attributes of the system, Eosin Y donor at 60 μM , Rhodamine B as acceptor.

For the fluorescein and eosin Y system, the inner filter FRET predictions using the molar absorptivities from the Jiang paper seem to explain the FRET signal seen. The predictions made using our absorbance's however only explain part; in the systems containing rhodamine B the FRET signal seen is more than predicted by either set of absorbance's, in fact it is almost double which could suggest a significant secondary inner filter effect (emission light being absorbed by a concentrated solution to the point that the light reaching the sensor is significantly reduced) although this has not been investigated. Predictions using the molar absorptivity from the absorbance data we collected and those made using the molar absorptivity from the Jiang paper gave differing results. The molar absorptivities calculated using our experimental data are lower than those in the Jiang paper and therefore the FRET predictions are lower. These differences are likely due to the difficulties measuring reverse micelle dye mixtures on a spectrophotometer; this is due to the high optical densities of the samples at the concentrations used in the study, absorbance measurements are most accurate when the values obtained about 0.1 to 1 absorbance units, at the concentrations in the paper in all the light is absorbed and thus the samples had to be diluted.

The approach in the Jiang paper was to reduce the overall dye concentration to $1\mu\text{M}$. Our approach was to dilute the samples to one tenth of their original concentration with isooctane, whilst avoiding reducing the surfactant concentration under the critical micelle concentration, this way the concentration of the dyes in the aqueous core of the reverse micelle remained comparable to those in the study, thus any dye concentration dependent effects, for instance dimer formation, at higher concentrations the formation of dimers is more likely, these would change the absorbance spectra of the solution and therefore the molar absorptivities calculated using that data. The solutions used to obtain the absorbance data were also read in a fluorimeter. Visual inspection of the spectra do not show any sign of peaks which are not present in the solutions of lone dyes. Only the visible region had clear enough data for this to be possible. Due to the absorbance of AOT in the UV it is unlikely that a suitable percentage of light was able to pass through the sample in this region.

The fluorescence and absorbance data was then compared to establish whether the changes in the absorbance explain the changes in fluorescence intensity. The fluorescent intensity or absorbance of the sample in each pair with the lowest acceptor concentration was used as a unit of one and it was

assumed they would increase linearly with concentration. Each sample was then compared to these predicted values. The experimental values divided by these predicted values are plotted in Figure 34, Figure 35 and Figure 36.

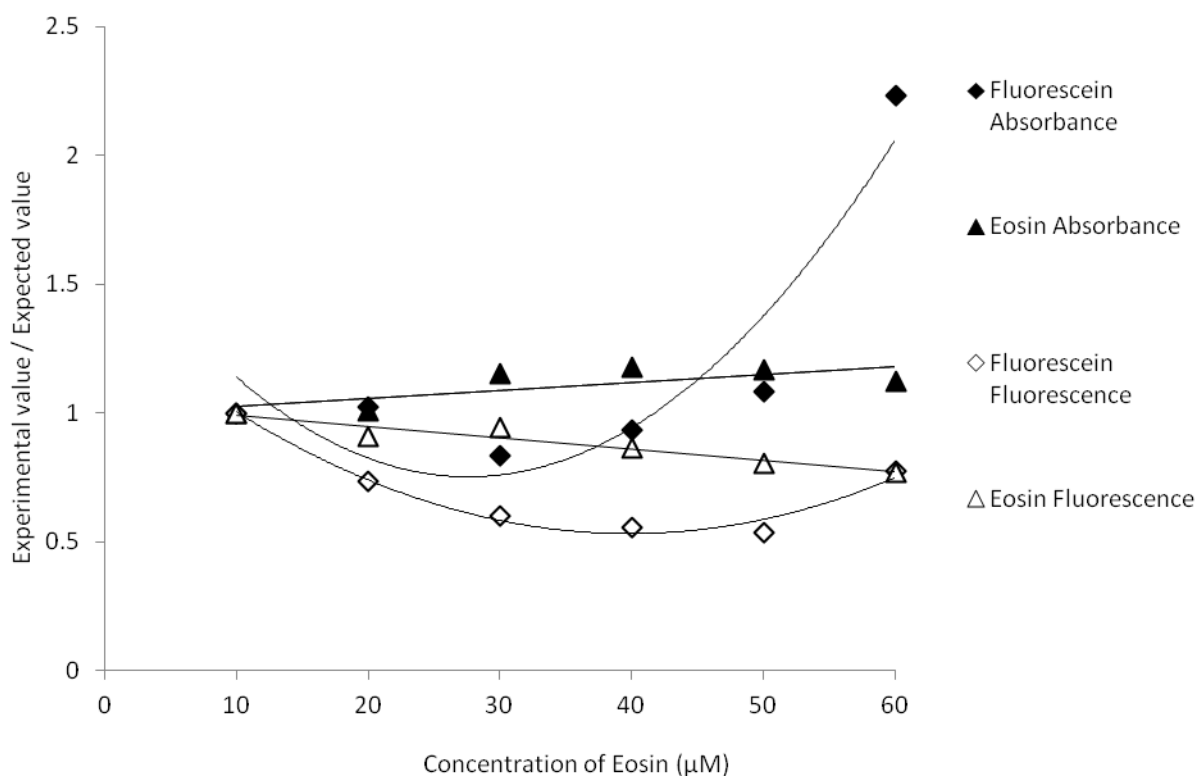


Figure 34: Comparison of experimental and expected values for fluorescence and absorbance, Fluorescein donor at 20μM, eosin Y as acceptor.

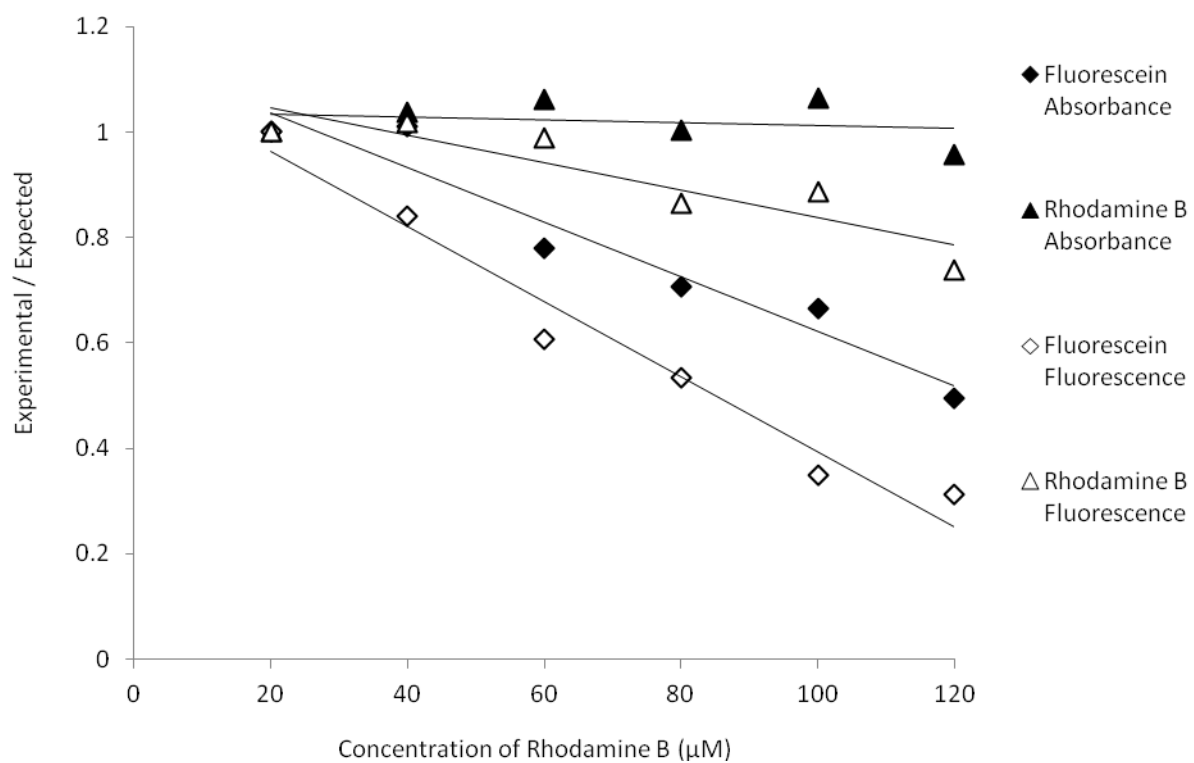


Figure 35: Comparison of experimental and expected values for fluorescence and absorbance, Fluorescein donor at 20μM, Rhodamine B as acceptor.

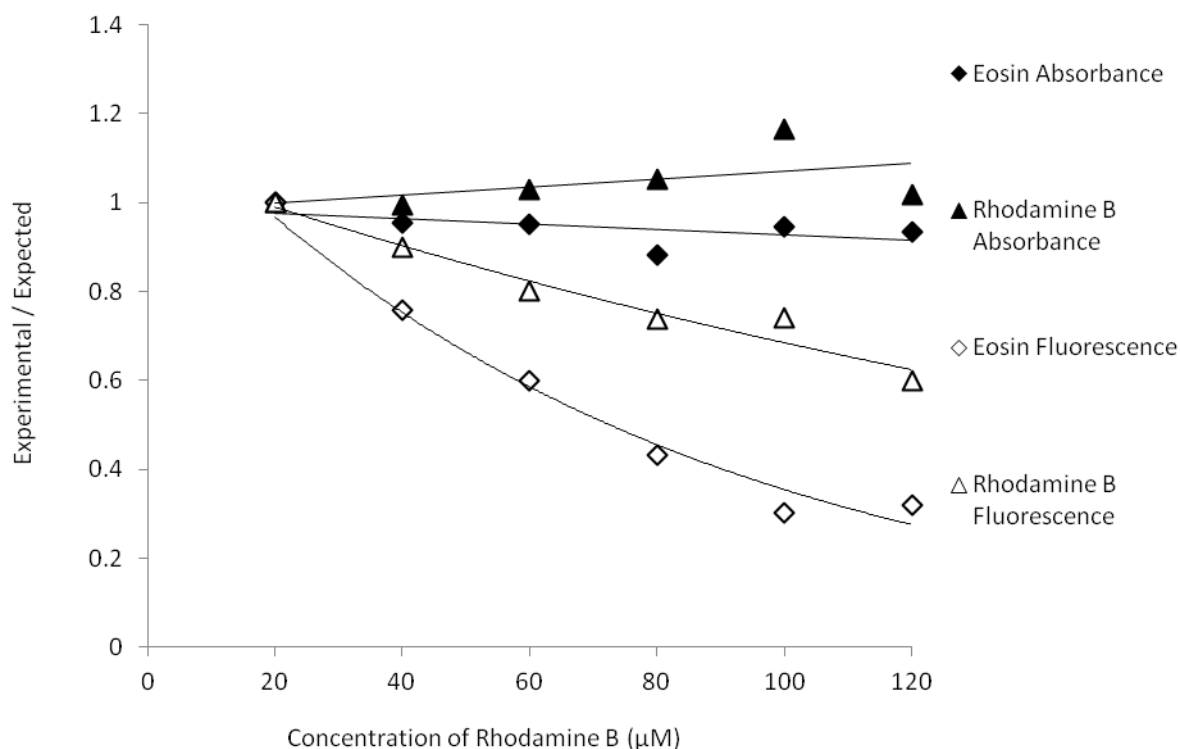


Figure 36: Comparison of experimental and expected values for fluorescence and absorbance, Eosin Y donor at $60\mu\text{M}$, Rhodamine B as acceptor.

For the fluorescein and eosin Y system in the absorbance data tends to remain at about 1 and therefore is changing as expected. The eosin Y fluorescence shows a slight steady decline as a concentration increases which may suggest secondary inner filter effects. Fluorescein's fluorescence is also reduced compared to the expected as the concentration of eosin Y increases, the last point shows a large increase in absorbance, and a slight increase in fluorescence. The fluorescein and rhodamine B pair show a clear decrease in the fluorescein absorbance and fluorescence suggesting that this reduction in absorbance is responsible for some of the reduction in intensities seen. There is also a slight reduction in the rhodamine B fluorescence but its absorbance does not show the clear downward trend seen in the fluorescein. The reduction in fluorescein absorbance could possibly suggest the formation of a dimer or possibly ion pairing with the rhodamine B which could possibly explain its decrease in fluorescence. The rhodamine B and eosin Y pair both show a clear decrease in fluorescence but no clear matching decrease in the absorbance. Their absorbencies stay close to be expected values. Eosin Y and rhodamine B will also be capable of forming an ion pair or possibly

dimers. However both of these would be expected to affect the absorption and this is not seen in this data (Chambers et al., 1974; Muto, 1976; López Arbeloa and Ruiz Ojeda, 1982; Jones et al., 1984; Fornasiero and Kurucsev, 1986; Ilich et al., 1996; Dare-Doyen et al., 2003; Bhowmik and Ganguly, 2005; De et al., 2005; Ghasemi et al., 2005; Setiawan et al., 2010).

The data refuting the possibility of significant levels of FRET we have looked at so far was taken from the binary systems, however the main aim of the Jiang paper was to look into a system containing three dyes system, which makes it possible that their statement of FRET was occurring in fact only applied to this three dye system. The unmixing of a three dye system is difficult especially if the dyes are interacting, instead we used an AB plot showing the data from 519nm to 682nm to look at the possibility of FRET here. The resulting plot can be seen in Figure 37.

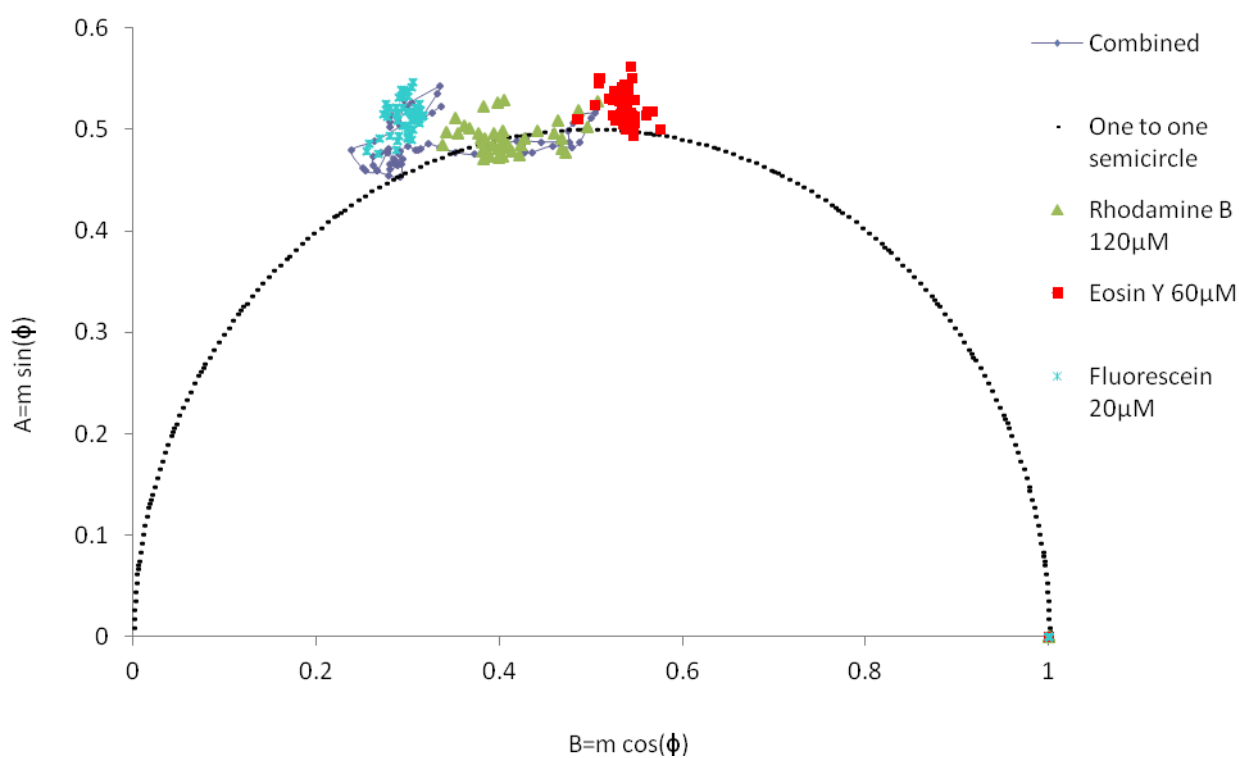


Figure 37: AB plot of the data points generated by the lone dyes in reverse micelles and the points generated when they are combined in the same reverse micelles.

The AB plot (Figure 37) shows no signs of FRET; if FRET was occurring then the points relating to the combined system would be expected to move away from the clusters of points relating to the lone dyes. This is clearly not the case as the data points of all the dyes combined occupy almost exactly the same space as the rhodamine B and fluorescein data points.

Interestingly none of the combined data points reach the lone eosin Y points; this suggests that in a mixture there is no set of wavelengths in which solely the eosin Y lifetime is present. This is suitable as at the emission maximum of the eosin Y is still significant fluorescence from both rhodamine B and fluorescein, whereas rhodamine B is the sole significant emitter at the longest wavelength and fluorescein is the sole emitter at the shortest (fluorescein shows a marked increase of the wavelength of its maximum emission in reverse micelles (Sjöback et al., 1995; De, 2004) , and thus the eosin Y emissions always end up being part of a multi-exponential decay. It is possible that this is true for rhodamine B as well and the fact that it performs a line of points rather than a cluster disguises the fact (the literature suggests that in certain situations it can have a single-exponential fluorescence decay of $1.74\text{s} \pm 0.02$ in water (Boens et al., 2007)). The points at (1,0) are the result of data clipping due to the intensity being below the required threshold to avoid overwhelming noise contamination, the software we use to extract the phase modulation lifetimes outputs these lifetimes as zero and running through the AB plot calculations gives the coordinates (1, 0). The combined data has no points under the threshold for this data range.

5. Conclusion

5.1 The microscope system

The system now seems almost capable of the measurements required for hunt for oligomers in GPCRS. The main requirement now for the imaging of cells in the system is a more powerful light source; a laser has been purchased for this purpose. It should also help deal with the background problems because of the shorter exposure times.

5.2 The model system

A robust model system for FRET is still very much required. The evidence produced by this work is strongly suggests that there is no significant FRET present in any of the dye combinations used in the Jiang paper and definite not enough to test a FRET predicting equation robustly. Using intensities to predict levels of FRET to be inherently difficult due to the large number of processes which can affect levels of the emission.

5.3 Why the model system is broken

The most clearly visible from our experiments is the inner filter effect. This explains a significant amount of the intensity reductions seen in the donors. However in certain cases it does not explain all. In these cases is believed that some form of dimer formation due to the high concentrations used at the propensity of these dyes to form dimers, however it's difficult to say whether dimers are present and if these dimers are hetero or homo dimers. The most obvious expected evidence would be changes in the absorption, this was not seen however the iso-octane absorbed heavily in the UV spectra making it difficult to see any changes there (Kajiwara et al., 1973). However it is also possible that these differences are due to a secondary inner filter effect resulting in the emitted light being absorbed by the solution. This effect proved difficult to model due to the fact that in a system designed to produce FRET there are large overlaps of the emission and absorption spectrums by design meaning that concentrated solution could end up having multiple absorption and re-emission events on the lights way out the system, potentially quantum yield and estimations of the likely number of absorption and re-emission events to be used to calculate the level of secondary inner

filter effects. This would require knowledge of the light intensity and spectral distribution of the light source entering the sample. Due to our use of an LED it is difficult to measure because of the necessity to measure at that point of entrance to get accurate usable value. Due to the collimated beam of a laser it may be possible to do it using a laser as the source although it's still likely to be difficult. It is interesting however that they get such good correlation and suggests that the calculations they have used to attempt to predict FRET could be adapted to instead predict these other processes. This makes me suspect that the inner filter effect is the key problem. The calculations to establish inner filter effects taking into account not just the primary effects I calculated but the secondary effects too would require very similar data to make a prediction, they may have accidentally stumbled upon an effective system for predicting the fluorescence of optically dense mixtures of non-interacting fluorophores without the aforementioned excitation source issues. It was established that a static process is responsible for the reduction in intensity because if it was dynamic then it would affect the lifetimes as well. Although the in-depth analysis was done on the unbuffered system, the buffered and unbuffered systems had clear differences in both lifetimes and intensities. Looking into these differences were within a reverse micelle system could make for interesting further work. Eosin Y in particular show large changes depending on buffering and this pH dependence seems less well-characterised than it is in say fluorescein (Klonis and Sawyer, 2000; Hammer et al., 2005; Mchedlov-Petrosyan et al., 2010). The high concentrations used in the study made it difficult to get accurate absorption data. The normal course of action - to dilute the sample - could be interpreted in different ways. This may have led to the differences between the absorbencies measured by us and those in the Jiang paper however simple experimental error was likely also a factor. A possible solution to the concentration problem would be to use ultrashort path flow cells which are better able to deal with high optical densities. This study shows the importance of confirming measurements using different methods if at all possible, with access to only the intensity data FRET seemed a perfectly reasonable explanation of the data however with the addition of lifetime data, a very different story has been told.

References

- Abel, S., Sterpone, F., Bandyopadhyay, S., and Marchi, M. (2004). Molecular Modeling and Simulations of AOT–Water Reverse Micelles in Isooctane: Structural and Dynamic Properties. *The Journal of Physical Chemistry B* *108*, 19458–19466.
- Abramoff, M.D., Magalhães, P.J., and Ram, S.J. (2004). Image processing with ImageJ. *Biophotonics International* *11*, 36–42.
- Battersby, B.J., Bryant, D., Meutermans, W., Matthews, D., Smythe, M.L., and Trau, M. (2000). Toward Larger Chemical Libraries: Encoding with Fluorescent Colloids in Combinatorial Chemistry. *Journal of the American Chemical Society* *122*, 2138–2139.
- Battersby, B.J., Lawrie, G.A., Johnston, A.P.R., and Trau, M. (2002). Optical barcoding of colloidal suspensions: applications in genomics, proteomics and drug discovery. *Chem. Commun.* 1435–1441.
- Bhowmik, B.B., and Ganguly, P. (2005). Photophysics of xanthene dyes in surfactant solution. *Spectrochimica Acta Part A: Molecular and Biomolecular Spectroscopy* *61*, 1997–2003.
- Bigelow, C.E., Vishwasrao, H.D., Frelinger, J.G., and Foster, T.H. (2004). Imaging enzyme activity with polarization-sensitive confocal fluorescence microscopy. *Journal of Microscopy* *215*, 24–33.
- Boens, N., Qin, W., Basarić, N., Hofkens, J., Ameloot, M., Pouget, J., Lefèvre, J.-P., Valeur, B., Gratton, E., vandeVen, M., et al. (2007). Fluorescence Lifetime Standards for Time and Frequency Domain Fluorescence Spectroscopy. *Analytical Chemistry* *79*, 2137–2149.
- Boite, S., and Cordelières, F.P. (2006). A guided tour into subcellular colocalization analysis in light microscopy. *Journal of Microscopy* *224*, 213–232.
- Canals, M., Marcellino, D., Fanelli, F., Ciruela, F., de Benedetti, P., Goldberg, S.R., Neve, K., Fuxe, K., Agnati, L.F., Woods, A.S., et al. (2003). Adenosine A2A-Dopamine D2 Receptor-Receptor Heteromerization: Qualitative And Quantitative Assessment By Fluorescence And Bioluminescence Energy Transfer. *J. Biol. Chem.* *278*, 46741–46749.
- Cao, Y., Sun, W.-C., Jin, L., Xie, K.-Q., and Zhu, X.-Z. (2006). Activation of adenosine A1 receptor modulates dopamine D1 receptor activity in stably cotransfected human embryonic kidney 293 cells. *European Journal of Pharmacology* *548*, 29–35.
- Carrillo, J.J., Padiani, J., and Milligan, G. (2003). Dimers of Class A G Protein-coupled Receptors Function via Agonist-mediated Trans-activation of Associated G Proteins. *J. Biol. Chem.* *278*, 42578–42587.
- Chambers, R.W., Kajiwarra, T., and Kearns, D.R. (1974). Effect of dimer formation on the electronic absorption and emission spectra of ionic dyes. Rhodamines and other common dyes. *The Journal of Physical Chemistry* *78*, 380–387.

- Cheng, Z.-J., and Miller, L.J. (2001). Agonist-dependent Dissociation of Oligomeric Complexes of G Protein-coupled Cholecystokinin Receptors Demonstrated in Living Cells Using Bioluminescence Resonance Energy Transfer. *J. Biol. Chem.* *276*, 48040–48047.
- Ciruela, F., Escriche, M., Burgueno, J., Angulo, E., Casado, V., Soloviev, M.M., Canela, E.I., Mallol, J., Chan, W.-Y., Lluís, C., et al. (2001). Metabotropic Glutamate 1 α and Adenosine A1 Receptors Assemble into Functionally Interacting Complexes. *J. Biol. Chem.* *276*, 18345–18351.
- Clayton, A.H.A., Hanley, Q.S., and Verveer, P.J. (2004). Graphical representation and multicomponent analysis of single-frequency fluorescence lifetime imaging microscopy data. *Journal of Microscopy* *213*, 1–5.
- Dare-Doyen, S., Doizi, D., Guilbaud, P., Djedaini-Pilard, F., Perly, B., and Millie, P. (2003). Dimerization of Xanthene Dyes in Water: Experimental Studies and Molecular Dynamic Simulations. *The Journal of Physical Chemistry B* *107*, 13803–13812.
- De, S. (2004). Fluorescence resonance energy transfer—a spectroscopic probe for organized surfactant media. *Journal of Colloid and Interface Science* *271*, 485–495.
- De, S., Das, S., and Girigoswami, A. (2005). Environmental effects on the aggregation of some xanthene dyes used in lasers. *Spectrochimica Acta Part A: Molecular and Biomolecular Spectroscopy* *61*, 1821–1833.
- Digman, M.A., Caiolfa, V.R., Zamaï, M., and Gratton, E. (2008). The phasor approach to fluorescence lifetime imaging analysis. *Biophys. J* *94*, L14–16.
- Dinger, M.C., Bader, J.E., Kobor, A.D., Kretzschmar, A.K., and Beck-Sickinger, A.G. (2003). Homodimerization of Neuropeptide Y Receptors Investigated by Fluorescence Resonance Energy Transfer in Living Cells. *J. Biol. Chem.* *278*, 10562–10571.
- Dunwiddie, T.V., and Masino, S.A. (2001). The role and regulation of adenosine in the central nervous system. *Annu Rev Neurosci* *24*, 31–55.
- Duysens, L.N. (1956). The flattening of the absorption spectrum of suspensions, as compared to that of solutions. *Biochim. Biophys. Acta* *19*, 1–12.
- Emmanuel, H. (2003). Biochemical and pharmacological control of the multiplicity of coupling at G-protein-coupled receptors. *Pharmacology & Therapeutics* *99*, 25–44.
- Ferguson, S.S.G. (2001). Evolving Concepts in G Protein-Coupled Receptor Endocytosis: The Role in Receptor Desensitization and Signaling. *Pharmacol Rev* *53*, 1–24.
- Florentini, C., Gardoni, F., Spano, P., Di Luca, M., and Missale, C. (2003). Regulation of Dopamine D1 Receptor Trafficking and Desensitization by Oligomerization with Glutamate N-Methyl-D-aspartate Receptors. *J. Biol. Chem.* *278*, 20196–20202.
- Fornasiero, D., and Kurucsev, T. (1986). Vibronic exciton bands. Absorption spectra of Eosin Y dimers. *J. Chem. Soc., Faraday Trans. 2* *82*, 15–19.
- Franco, R., Ferré, S., Agnati, L., Torvinen, M., Ginés, S., Hillion, J., Casadó, V., Lledó, P.-M., Zoli, M., Lluís, C., et al. (2000). Evidence for Adenosine/Dopamine Receptor Interactions: Indications for Heteromerization. *Neuropsychopharmacology* *23*, S50–S59.

- Gautier, I., Tramier, M., Durieux, C., Coppey, J., Pansu, R.B., Nicolas, J.C., Kemnitz, K., and Coppey-Moisan, M. (2001). Homo-FRET microscopy in living cells to measure monomer-dimer transition of GFP-tagged proteins. *Biophys J.* *80*, 3000–3008.
- Ghasemi, J., Niazi, A., and Kubista, M. (2005). Thermodynamics study of the dimerization equilibria of rhodamine B and 6G in different ionic strengths by photometric titration and chemometrics method. *Spectrochim Acta A Mol Biomol Spectrosc* *62*, 649–656.
- Ginés, S., Hillion, J., Torvinen, M., Le Crom, S., Casadó, V., Canela, E.I., Rondin, S., Lew, J.Y., Watson, S., Zoli, M., et al. (2000). Dopamine D1 and adenosine A1 receptors form functionally interacting heteromeric complexes. *Proceedings of the National Academy of Sciences of the United States of America* *97*, 8606–8611.
- Goel, T., Kumbhakar, M., Mukherjee, T., and Pal, H. (2010). Effect of sphere to rod transition on the probe microenvironment in sodium dodecyl sulphate micelles: A time resolved fluorescence anisotropy study. *Journal of Photochemistry and Photobiology A: Chemistry* *209*, 41–48.
- Gsandtner, I., Charalambous, C., Stefan, E., Ogris, E., Freissmuth, M., and Zetzl, J. (2005). Heterotrimeric G Protein-independent Signaling of a G Protein-coupled Receptor. *J. Biol. Chem.* *280*, 31898–31905.
- Hammer, M., Schweitzer, D., Richter, S., Königsdörfer, E., and Riederer, E. (2005). Sodium fluorescein as a retinal pH indicator? *Physiological Measurement* *26*, N9–N12.
- Hanley, Q.S., Arndt-Jovin, D.J., and Jovin, T.M. (2002). Spectrally Resolved Fluorescence Lifetime Imaging Microscopy. *Appl. Spectrosc.* *56*, 155–166.
- Hanley, Q.S., and Clayton, A.H.A. (2005). AB-plot assisted determination of fluorophore mixtures in a fluorescence lifetime microscope using spectra or quenchers. *J Microsc* *218*, 62–67.
- Hanley, Q.S., Murray, P.I., and Forde, T.S. (2006). Microspectroscopic fluorescence analysis with prism-based imaging spectrometers: Review and current studies. *Cytometry Part A* *69A*, 759–766.
- Hanley, Q.S., Subramaniam, V., Arndt-Jovin, D.J., and Jovin, T.M. (2001). Fluorescence lifetime imaging: multi-point calibration, minimum resolvable differences, and artifact suppression. *Cytometry* *43*, 248–260.
- Hoffmann, C., Gaietta, G., Bunemann, M., Adams, S.R., Oberdorff-Maass, S., Behr, B., Vilardaga, J.-P., Tsien, R.Y., Ellisman, M.H., and Lohse, M.J. (2005). A FIAsh-based FRET approach to determine G protein-coupled receptor activation in living cells. *Nat Meth* *2*, 171–176.
- Ilich, P., Mishra, P.K., Macura, S., and Burghardt, T.P. (1996). Direct observation of rhodamine dimer structures in water. *Spectrochimica Acta Part A: Molecular and Biomolecular Spectroscopy* *52*, 1323–1330.
- Jiang, Y., Borrelli, L., Bacskai, B.J., Kanaoka, Y., and Boyce, J.A. (2009). P2Y6 Receptors Require an Intact Cysteinyl Leukotriene Synthetic and Signaling System to Induce Survival and Activation of Mast Cells. *J Immunol* *182*, 1129–1137.

- Jiang, Z.-J., and Goedel, W.A. (2008). Fluorescence properties of systems with multiple Forster transfer pairs. *Phys. Chem. Chem. Phys.* *10*, 4584–4593.
- Johansson, M.K., and Cook, R.M. (2003). Intramolecular Dimers: A New Design Strategy for Fluorescence-Quenched Probes. *Chemistry - A European Journal* *9*, 3466–3471.
- Jones, G.R., Duddell, D.A., Murray, D., Cundall, R.B., and Catterall, R. (1984). Eosin Y-macromolecule complexes. Part 1.-Application of exciton theory to the study of the arrangement of eosin Y molecules in polycation-induced eosin Y dimers. *J. Chem. Soc., Faraday Trans. 2* *80*, 1181–1199.
- Jones, K.A., Borowsky, B., Tamm, J.A., Craig, D.A., Durkin, M.M., Meng Dai, Wen-Jeng Yao, Johnson, M., Gunwaldsen, C., Ling-Yan Huang, et al. (1998). GABAB receptors function as a heteromeric assembly of the subunits GABABR1 and GABABR2. *Nature* *396*, 674.
- Jordan, B.A., and Devi, L.A. (1999). G-protein-coupled receptor heterodimerization modulates receptor function. *Nature* *399*, 697–700.
- Kajiwara, T., Chambers, R.W., and Kearns, D.R. (1973). Dimer spectra of rhodamine B. *Chemical Physics Letters* *22*, 37–40.
- Kaupmann, K., Malitschek, B., Schuler, V., Heid, J., Froesti, W., Beck, P., Mosbacher, J., Bischoff, S., Kulik, A., Shigemoto, R., et al. (1998). GABAB-receptor subtypes assemble into functional heteromeric complexes. *Nature* *396*, 683.
- Klonis, and Sawyer (2000). Effect of solvent-water mixtures on the prototropic equilibria of fluorescein and on the spectral properties of the monoanion. *Photochem. Photobiol.* *72*, 179–185.
- Kuner, R., Kohr, G., Grunewald, S., and Kornau, H.-C. (1999). Role of Heteromer Formation in GABA B Receptor Function. *Science* *283*, 74.
- Lakowicz, J.R. (1999). *Principles of Fluorescence Spectroscopy* (New York: Kluwer Academic/Plenum Publishers).
- Lidke, D.S., Nagy, P., Barisas, B.G., Heintzmann, R., Post, J.N., Lidke, K.A., Clayton, A.H.A., Arndt-Jovin, D.J., and Jovin, T.M. (2003). Imaging molecular interactions in cells by dynamic and static fluorescence anisotropy (rFLIM and emFRET). *Biochem Soc Trans* *31*, 1020–1027.
- López Arbeloa, I., and Ruiz Ojeda, P. (1982). Dimeric states of rhodamine B. *Chemical Physics Letters* *87*, 556–560.
- Lopez-Gimenez, J.F., Canals, M., Pediani, J.D., and Milligan, G. (2007). The $\alpha 1b$ -Adrenoceptor Exists as a Higher-Order Oligomer: Effective Oligomerization Is Required for Receptor Maturation, Surface Delivery, and Function. *Mol Pharmacol* *71*, 1015–1029.
- Maggio, R., Vogel, Z., and Wess, J. (1993). Coexpression studies with mutant muscarinic/adrenergic receptors provide evidence for intermolecular “cross-talk” between G-protein-linked receptors. *Proceedings of the National Academy of Sciences of the United States of America* *90*, 3103–3107.
- Marrero M, Venema V, Ju H, He H, Liang H, Caldwell R, and Venema R (1999). Endothelial nitric oxide synthase interactions with G-protein-coupled receptors. *Biochem J.* *343*, 335–340.

- Mchedlov-Petrosyan, N.O., Vodolazkaya, N.A., Gurina, Y.A., Sun, W.-C., and Gee, K.R. (2010). Medium Effects on the Prototropic Equilibria of Fluorescein Fluoro Derivatives in True and Organized Solution. *The Journal of Physical Chemistry B* *114*, 4551–4564.
- Muto, J. (1976). Dimeric properties of Rhodamine B in glycerol, ethylene glycol, and acetic acid. *The Journal of Physical Chemistry* *80*, 1342–1346.
- Nimchinsky, E.A., Hof, P.R., Janssen, W.G.M., Morrison, J.H., and Schmauss, C. (1997). Expression of Dopamine D3 Receptor Dimers and Tetramers in Brain and in Transfected Cells. *J. Biol. Chem.* *272*, 29229–29237.
- Pfeiffer, M., Kirscht, S., Stumm, R., Koch, T., Wu, D., Laugsch, M., Schröder, H., Höllt, V., and Schulz, S. (2003). Heterodimerization of Substance P and μ -Opioid Receptors Regulates Receptor Trafficking and Resensitization. *J. Biol. Chem.* *278*, 51630–51637.
- Ramsay, D., Kellett, E., McVey, M., Rees, S., and Milligan, G. (2002). Homo- and hetero-oligomeric interactions between G-protein-coupled receptors in living cells monitored by two variants of bioluminescence resonance energy transfer (BRET): hetero-oligomers between receptor subtypes form more efficiently than between less closely related sequences. *Biochem J* *365*, 429–440.
- Redford, G., and Clegg, R. (2005). Polar Plot Representation for Frequency-Domain Analysis of Fluorescence Lifetimes. *Journal of Fluorescence* *15*, 805–815.
- Rocheville, M., Lange, D.C., Kumar, U., Patel, S.C., Patel, R.C., and Patel, Y.C. (2000a). Receptors for Dopamine and Somatostatin: Formation of Hetero-Oligomers with Enhanced Functional Activity. *Science* *288*, 154.
- Rocheville, M., Lange, D.C., Kumar, U., Sasi, R., Patel, R.C., and Patel, Y.C. (2000b). Subtypes of the Somatostatin Receptor Assemble as Functional Homo- and Heterodimers. *J. Biol. Chem.* *275*, 7862–7869.
- Salim, K., Fenton, T., Bacha, J., Urien-Rodriguez, H., Bonnert, T., Skynner, H.A., Watts, E., Kerby, J., Heald, A., Beer, M., et al. (2002). Oligomerization of G-protein-coupled Receptors Shown by Selective Co-immunoprecipitation. *J. Biol. Chem.* *277*, 15482–15485.
- Schlyer, S., and Horuk, R. (2006). I want a new drug: G-protein-coupled receptors in drug development. *Drug Discov Today* *11*, 481–493.
- Setiawan, D., Kazaryan, A., Martoprawiro, M.A., and Filatov, M. (2010). A first principles study of fluorescence quenching in rhodamine B dimers: how can quenching occur in dimeric species? *Phys. Chem. Chem. Phys.* *12*, 11238.
- Sjöback, R., Nygren, J., and Kubista, M. (1995). Absorption and fluorescence properties of fluorescein. *Spectrochimica Acta Part A: Molecular and Biomolecular Spectroscopy* *51*, L7–L21.
- Tawfik, H.E., Schnermann, J., Oldenburg, P.J., and Mustafa, S.J. (2005). Role of A1 adenosine receptors in regulation of vascular tone. *Am J Physiol Heart Circ Physiol* *288*, H1411–1416.
- Vasquez, V.R., Williams, B.C., and Graeve, O.A. (2011). Stability and Comparative Analysis of AOT/Water/Isooctane Reverse Micelle System Using Dynamic Light Scattering and Molecular Dynamics. *The Journal of Physical Chemistry B* *115*, 2979–2987.

- Verveer, P.J., and Hanley, Q.S. (2009). Frequency Domain FLIM Theory, Instrumentation and Data Analysis.
- Wittung, P., Kajanus, J., Kubista, M., and Malmström, B.G. (1994). Absorption flattening in the optical spectra of liposome-entrapped substances. *FEBS Lett* 352, 37–40.
- Wong, S.K.-F. (2003). G Protein Selectivity Is Regulated by Multiple Intracellular Regions of GPCRs. *Neurosignals* 12, 1–12.
- Wyatt, W.A., Poirier, G.E., Bright, F.V., and Hieftje, G.M. (1987). Fluorescence spectra and lifetimes of several fluorophores immobilized on nonionic resins for use in fiber-optic sensors. *Analytical Chemistry* 59, 572–576.
- Xu, J., He, J., Castleberry, A.M., Balasubramanian, S., Lau, A.G., and Hall, R.A. (2003). Heterodimerization of $\alpha 2A$ - and $\beta 1$ -Adrenergic Receptors. *J. Biol. Chem.* 278, 10770–10777.
- Yeow, E.K.L., and Clayton, A.H.A. (2007). Enumeration of oligomerization states of membrane proteins in living cells by homo-FRET spectroscopy and microscopy: theory and application. *Biophys J* 92, 3098–3104.
- Yoshioka, K., Hosoda, R., Kuroda, Y., and Nakata, H. (2002a). Hetero-oligomerization of adenosine A1 receptors with P2Y1 receptors in rat brains. *FEBS Letters* 531, 299–303.
- Yoshioka, K., Saitoh, O., and Nakata, H. (2001). Heteromeric association creates a P2Y-like adenosine receptor. *Proceedings of the National Academy of Sciences of the United States of America* 98, 7617–7622.
- Yoshioka, K., Saitoh, O., and Nakata, H. (2002b). Agonist-promoted heteromeric oligomerization between adenosine A1 and P2Y1 receptors in living cells. *FEBS Letters* 523, 147–151.
- Zhou, Y., Dickenson, J.M., and Hanley, Q.S. (2009). Imaging lifetime and anisotropy spectra in the frequency domain. *Journal of Microscopy* 234, 80–88.